The ontogeny of immune tolerance: a model of early-life secretory IgA - gut microbiome interactions

Burcu Tepekule[1*], Ai Ing Lim[2], C. Jessica E. Metcalf[1*]

[1] Dept of Ecology and Evolutionary Biology, Princeton University, Princeton, 08544, USA.
[2] Dept of Molecular Biology, Princeton University, Princeton, 08544, USA.

*Corresponding authors. Emails: burcutepekule@gmail.com, cjmetcalf@princeton.edu

Abstract: To achieve immune and microbial homeostasis during adulthood, the developing immune system must learn to identify which microbes to tolerate and which to defend against. How such 'immune education' unfolds remains a major knowledge gap. We address this gap by synthesizing existing literature to develop a mechanistic mathematical model representing the interplay between gut ecology and adaptive immunity in early life. Our results indicate that the inflammatory tone of the microenvironment is the mediator of information flow from pre- to post-weaning periods. We evaluate the power of postnatal fecal samples for predicting immunological trajectories and explore breastfeeding scenarios when maternal immunological conditions affect breastmilk composition. Our work establishes a quantitative basis for 'immune education', yielding insights into questions of applied relevance.

Main Text:

Introduction

The global burden of immune-mediated disease is rapidly growing [1]. Epidemiological data indicate that early life exposures are key determinants of immune-mediated diseases later in life [2], such as allergies [3], asthma [4], type 1 diabetes [5], and inflammatory bowel disease (IBD) [6]. This impact of early life is primarily attributed to interactions between the microbiome and the immune system during a critical developmental window, which enables hosts to establish tolerance to commensal bacteria [7], ensuring the maintenance of immune and microbial homeostasis into adulthood, while appropriately defending against pathogens [8,9]. When this crosstalk is perturbed, pathological imprinting may develop, characterized by excessive immune reactivity and increased susceptibility to inflammatory diseases in adulthood [10]. Both inherent microbial factors and maternal cues determine how microbe-immune interactions unfold during early life: symbiotic commensals provide metabolic products that establish regulatory pathways facilitating a balanced immune response, whereas pathogens stimulate the immune system to develop defense mechanisms. Breastmilk delivers microbes and nutrients, but also antibodies that dictate the timing and nature of bacterial antigen presentation to the infant's developing immune system, establishing a transgenerational cycle of immune priming [11,12]. The collective influence of these processes on immune ontogeny and maturation is encapsulated by the term 'immune education' [13].

The information available to tackle the establishment of 'immune education' is now considerable [14]. To date, thousands of papers have been published, ranging from observational data from human populations to experimental perturbations in animal models. However, experimental methods inevitably focus on a limited set of mechanisms, while larger scale descriptive analysis

rooted in observational data may illuminate patterns, but ultimately yield verbal descriptions lacking mathematical characterization. The time is ripe to integrate these layers of evidence into a systems biology framework that formally accounts for the multiple potential interacting components. Such a foundation will open the way to generating testable hypotheses for empirical investigation based on experimental and clinical data, and further mechanistic modeling.

To this end, we introduce a mathematical framework describing the reciprocal imprinting of the human gut microbiome and the antigen-specific endogenous mucosal Secretory Immunoglobulin A (SIgA) response during the first two years of life. While immune outcomes are undoubtedly multifaceted and influenced by numerous factors, many lines of evidence indicate the importance of the SIgA response, as its reactivity to microbial antigens plays a crucial role in mediating gut immune responses and their dysregulation [15,16]. The SIgA response also integrates both the B-cell and T-cell arms of immune ontogeny, and manifests the dual functionality of the gut mucosal immune system by selectively neutralizing pathogens while tolerating commensal bacteria beneficial for immune homeostasis [17,18]. Furthermore, SIgA represents the transgenerational aspect of immune priming: maternal SIgA modulates antigen presentation while simultaneously regulating the gut community composition [11,19].

Our mechanistic modeling strategy (Fig. 1) blends flexibility with tractability in reflecting the effects of maternal factors, feeding practices, consumer resource dynamics within microbial communities, and multifunctionality of SIgA (Fig. 1B); and introduces a quasi-stochastic mathematical model of germinal center reactions embedded in a combination of ordinary and delay differential equations (Fig. 1C). We parameterize our framework using data from infant fecal samples [20–23], formally mapping microbial abundance measurements into expectations for the dynamics of the lumen and the germinal centers of the gut, contexts traditionally obscured by the impracticality of direct sampling [24] (Fig. 1A). The mechanistic model structure entails a high dimensional parameter space, but qualitative results are consistent across parameter combinations (Supplementary Materials, Global and Local Sensitivity Analyses).

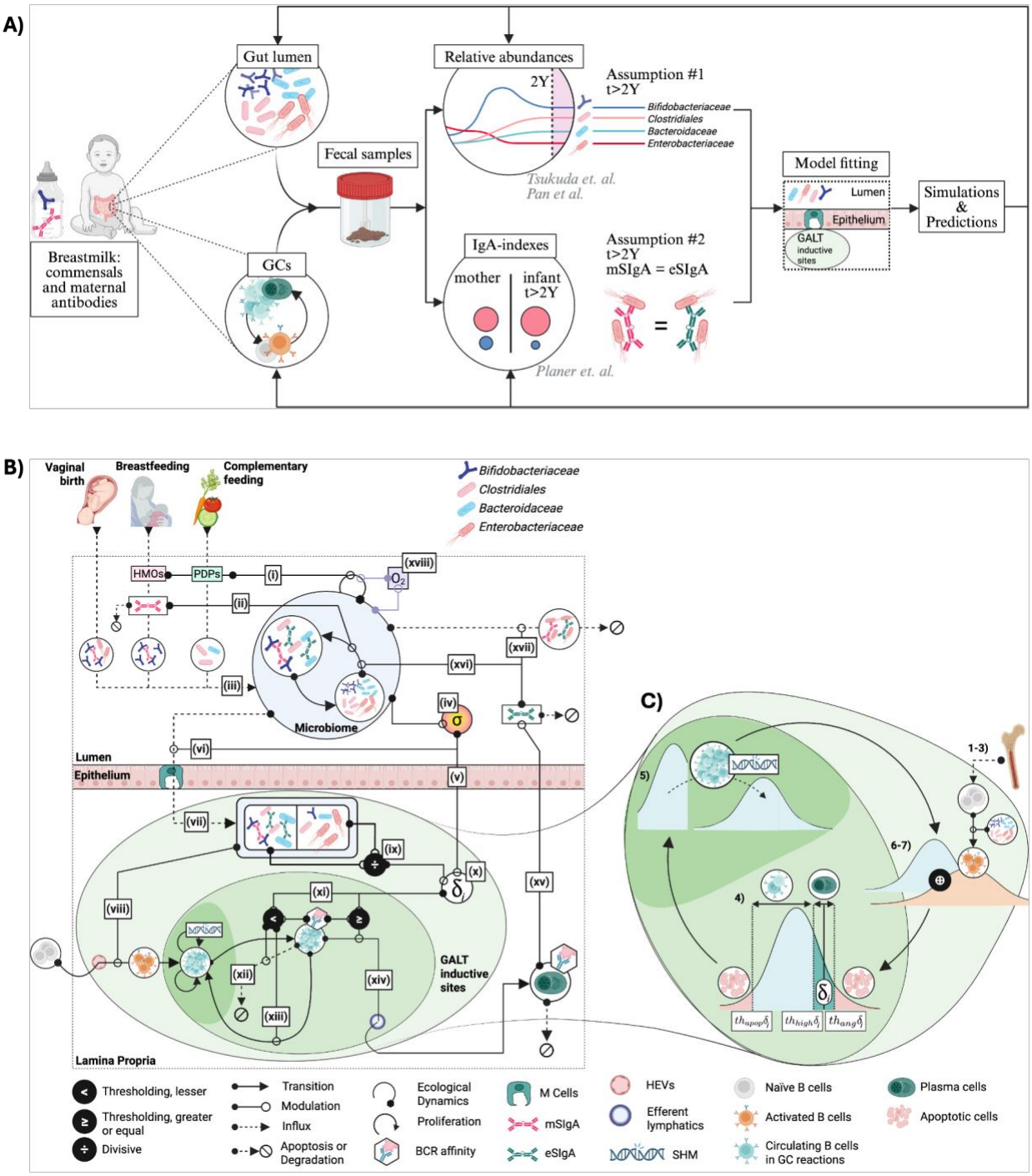

Fig 1. Modeling framework. A) Key data sources and assumptions used during model fitting, including relative abundance (line plot) and IgA-index (bubble plot) data, each colored by taxon. Model predictions reconstruct ecological dynamics in the gut lumen and the germinal center (GC) reactions. 2Y: 2 years; mSIgA and eSIgA: maternal and endogenous secretory Immunoglobulin A. **B)** Model dynamics. **(i)** Breastfeeding and complementary feeding introduces human milk oligosaccharides (HMOs), plant-derived polysaccharides (PDPs), **(ii)** mSIgA, and **(iii)** commensal bacteria to the gut lumen as SIgA-bacteria complexes or bacteria alone, alongside with the bacteria seeding the infant's gut during vaginal birth. The microbiome within the gut lumen (large light

blue circle), contains subpopulations of commensals that exist either in an SIgA-bound (white circle, left) or unbound (white circle, right) state, and transition between the two is driven by SIgA coating or degradation. **(iv)** Bacterial populations modulate the inflammatory tone of the microenvironment of the gut lumen (σ), **(v)** influencing epithelial cell-mediated communication with the organized gut-associated lymphoid tissue (GALT) inductive sites, and **(vi)** the antigenic sampling through barrier integrity. **(vii)** SIgA-bound and unbound antigens sampled by Microfold (M) cells **(viii)** activate the naïve B cells, and **(ix)** drive the balance between antigen-specific regulatory versus helper T cells (indicated by the divide sign). **(x)** This balance and σ shape the selection threshold δ_i for taxon i, **(xi)** which determines the BCR affinity ranges that lead to different B cell fates: **(xii)** apoptosis, **(xiii)** continued circulation, or **(xiv)** terminal differentiation into IgA-secreting plasma cells. **(xv)** IgA secreted by the plasma cells regulates the microbiome via **(xvi)** masking and **(xvii)** neutralization functions. Alongside the HMOs and PDPs, **(xviii)** the oxygen concentration (O_2) also influences the ecological dynamics based on commensals' metabolism. **C)** GC reactions (steps 1-7, materials and methods, corresponding to **(x)-(xiv)** on the previous panel). Naïve B cells with a wide BCR affinity distribution migrate from the bone marrow to the GALT inductive sites, and their affinity distribution is combined with that of circulating B-cells. B-cells activate upon encountering bacterial antigens. Based on how close their BCR affinities are to the selection threshold δ_i, cells undergo positive selection, receiving adequate T cell help to continue circulating or differentiate to IgA-secreting plasma cells; and if not, become apoptotic. Circulating cells undergo somatic hypermutation (SHM), increasing the standard deviation of their BCR affinity distribution, continuing the cycle.

Overall, our model brings mathematical formalism to the concept of 'immune education'. This framework enables us to explore three questions with translational implications. First, it supports the quantification of potentially key diagnostic markers; second, the simulation of clinical intervention strategies, and third, identification of preventive measures before pathological trajectories are imprinted. Overall, it allows us to systematically explore the emergent properties of this complex system in a controlled, interpretable, and reproducible setting. In doing so, it opens the way to investigating persistent questions in early-life immunology with both fundamental and applied relevance.

Results

Model outcomes unveil the dynamics in gut lumen, successfully predicting out-of-sample data

Capturing immune education requires encompassing exogenous inputs into the gut lumen alongside endogenous dynamics in the gut lumen and organized gut-associated lymphoid tissue (GALT) inductive sites such as Peyer's patches and colonic patches (Fig. 1A, see Table S4 for anatomical distinctions relevant to the model). Exogenous inputs quantified based on different feeding practices of infants [25–27] (Eqns. S1.1.18-S1.1.21), include caloric intake from human milk oligosaccharides (HMOs) and plant-derived polysaccharides (PDPs), and maternal secretory Immunoglobulin A (mSIgA) concentrations. HMOs and PDPs differentially modulate growth rates of different bacterial taxa based on their metabolism [28–32] (Eqn. S1.1.4). Timing of endogenous immune system activation is dictated by the maturation of Microfold (M) cells, which serve as the primary route for antigen transport to GALT inductive sites (Fig. 1B), the key site for the development of the gut adaptive immune response [33,34]. M cells are shown to appear shortly

before weaning in mice models, primarily due to decreasing concentrations of maternal steroids in breastmilk [35], for which we use mSIgA as a proxy, given a lack of quantitative data. While the timing of M cell maturation in humans remains unclear, we address this uncertainty through sensitivity analysis (Supplementary Materials, Local Sensitivity Analyses). M cell maturation translates into antigenic sampling — and thus the start of immune response maturation (Fig. 2A).

To fit our model to fecal microbiome data [20–23] and the established timeline of immune ontogeny [14,35], we leverage two observations: i) the infant develops an SIgA profile resembling their nursing mother's [21], and ii) the infant's immune response and microbial community structure stabilize after two years [33] (Fig. 1A). Specifically, the matured offspring secretes endogenous antibodies with quantitatively similar affinities to bacterial groups as their nursing mother; and relative abundances of bacterial taxa converge to their equilibrium values in host's fecal samples from day 720. We estimate a single set of affinity values shared between the mother and the matured offspring, reflecting maternal antibodies in the gut lumen before activation and after the stabilization of the host's immune response. For this step of inference, we define a composite optimization criterion that integrates the relative and absolute abundances of key taxonomic groups observed in fecal samples of infants and their IgA indexes (indicating enrichment in the SIgA coated (SIgA+) fractions). This optimization step provides estimates that remain fixed during the inference for the interim phase of endogenous immune system maturation. A second composite optimization criterion is applied to match the average SIgA coating ratio [36] in the gut lumen and the matured endogenous affinity values to the maternal ones.

To capture immunological and competitive interactions across ontogeny, we selected four bacterial taxonomic groups to reflect broad categories of host-bacterial interactions: *Enterobacteriaceae* encompasses the *Escherichia-Shigella* genus with potentially pathogenic [37,38] bacteria encountered pre-weaning when the endogenous system is more vulnerable to enteric infections. *Bifidobacteriaceae* represents early colonizers with anti-inflammatory properties that regulate the microenvironment and provide colonization resistance. *Bacteroidaceae* and *Clostridiales* are post-weaning bacteria with potentially anti-inflammatory properties that contribute to a balanced gut environment when properly regulated by SIgA (Table S2). Taxa are differentiated by two parameters: *i)* their invasiveness [39], defined as their potential to penetrate intestinal epithelial cells, and *ii)* their immunostimulatory potential, defined as their capacity to modulate the inflammatory tone of the microenvironment [40,41] via their metabolic products and epithelial conditioning [42]. While the relative ranking of these parameters across taxa is established *a priori* based on literature – for example, *Escherichia-Shigella* is assumed to have higher invasiveness and immunostimulatory potential than the rest of the taxa given its pathogenic potential – their specific values are inferred during model fitting (Table S3). Although bacterial niche (such as proximity to the epithelium [43]) could serve as an additional parameter for differentiating taxa in relation to SIgA responses, it has not been included in the model due to lack of existing quantitative data.

There is substantial evidence that the transfer of maternal antibodies to the infant gut through breastmilk plays a crucial role in shaping the neonatal gut microbiome and the immune system's development [19,44,45]. We characterize SIgA's functionality into two non-exclusive categories: masking (M), which represents SIgA's non-neutralizing functionality, promoting the intestinal residency of the symbiotic commensals by limiting their interactions with the immune system

[46,47]; and neutralizing (N), contributing to the expulsion of bacteria from the gut [43]. The masking (M) and neutralizing (N) rates per one unit of SIgA concentration are both modeled as a graduated response to affinity levels [48] (Eqn. S1.1.1-S1.1.2) based on the observation that SIgA targeting pathogens or pathobionts generally exhibits higher affinity compared to SIgA targeting symbiotic commensals, which often neutralizes rather than promotes their presence [49]. These rates are scaled by the binding ability of the antibodies, which we define as the strength of association between an antibody and its target antigen based on its affinity (Eqn. S1.1.3). This dual function of SIgA creates three subpopulations in the gut lumen — uncoated (SIgA-), masked (SIgA+ (M)), and neutralized (SIgA+ (N)) — of which only the uncoated and masked are metabolically active. The neutralized subpopulation neither interacts with other subpopulations nor stimulates the immune system. Because both masked and neutralized populations are coated with SIgA, techniques like IgA-Seq or BugFACS would detect binding in both cases, and the resulting SIgA coating ratio would reflect contributions from both types of bacteria. Furthermore, the functional dichotomy between high-affinity neutralizing and low-affinity masking SIgA is not absolute, as SIgA binding can influence bacterial growth or colonization in species-specific ways, involving mechanisms such as enchained growth, biofilm formation, or altered gene expression [17]. Given the scale of data available, our model does not attempt to capture these nuances (see supplementary material, section *Model Limitations*), but instead focuses on a fundamental, bacteria-agnostic mechanism, aiming to capture the core features of SIgA-microbiome interactions. Rather than relying on species-specific rules, our framework explores how affinity and functionality shift dynamically under different physiological conditions such as homeostasis and inflammation.

Our model assumes a common set of mechanisms for endogenous SIgA maturation across all commensals, allowing rates of antibody masking and neutralization to emerge from maturing affinity levels, as shaped by a backdrop of time-varying processes including developmental stages and dietary patterns (Fig. 2A). Our quasi-stochastic formulation of germinal center reactions assumes a temporally dynamic distribution of B-cell receptor (BCR) binding variability that dictates B cell fates; mean and standard deviation of binding variability are adjusted at each proliferation, somatic hypermutation, and selection (P-SHM-S) cycle (Fig. 1C). Naïve B cells migrate to the GALT inductive sites, are activated depending on the antigen uptake by M cells (Eqns. S1.1.5-S1.1.7), and start participating in GC reactions [50]. Each P-SHM-S cycle is informed by the microenvironmental stimulation in the PPs, and the selection pressure imposed by an implicit model of antigen-specific follicular helper and regulatory T cells (Materials and Methods, *Modeling the role of Germinal Centres*, and Eqn. S1.2.8), eventually determining the size and average affinity of the plasma cell pool. Microenvironmental stimulation is modeled as a composite variable (Eqn. S1.1.8) reflecting the cumulative effects of cytokines and microbial products; akin to the inflammatory tone of the local environment [51]. We infer mSIgA affinities (Fig. 2B) assuming the nursing mother with a balanced microbiome-immune response transfers masking antibodies for the symbiotic commensals (*Bifidobacteriaceae*, *Bacteroidaceae* and *Clostridiales*); and neutralizing antibodies for the pathogenic taxon *Enterobacteriaceae* [48,52–56]. Model fit estimates illustrate the trajectory of microenvironmental stimulation (Fig. 2C), average affinity of the endogenous antibodies converging toward maternal values (Fig. 2D), along with the normalized concentrations of antibody levels (Fig. 2E) proportional to the maturation of plasma cells being imprinted as the host ages.

Bacterial colonization is also affected by the oxygen concentration (O_2) in the gut lumen (Eqn. S1.1.4). O_2 inhibits the growth of obligate anaerobic bacteria and is consumed by facultative anaerobes (Eqn. S1.2.3) [57]. From an initially normalized level of 1, O_2 degrades at a rate inferred during the model fitting process (Fig. 2C).

To parametrize our model, we use relative bacterial abundance and IgA-Seq data derived from infants' fecal samples [20–23] as a proxy for the ecological and immunological dynamics within the gut lumen [58]; however, equating fecal samples with the gut lumen overlooks SIgA's role in microbial turnover [46,47]. We reconstruct the relative abundances per fecal content by calculating the weighted sum of neutralized, coated, and uncoated subpopulations in the gut lumen. This calculation incorporates subpopulation-specific observation rates (Eqns. S1.1.14-S1.1.17), which represent the proportion of each bacterial subpopulation that successfully transfers from the gut lumen to fecal samples. These observation rates are inferred during the model fitting process and differ between neutralized, coated, and uncoated bacteria (Table S3), accounting for their varying propensities to appear in fecal samples relative to their actual abundance in the gut lumen. This approach translates the true microbial abundances in the gut lumen to the measurable abundances detected in fecal samples (Fig. 1A), allowing us to align the model output with the 16S rRNA sequencing analysis provided in *Tsukuda et al* [20]. We apply the same reconstruction using SIgA−, SIgA+(C), and SIgA+(N) subpopulations to compute the IgA indexes for each taxon, allowing us to include the IgA-seq profiles of *Enterobacteriaceae* and *Bifidobacteriaceae* provided in *Planer et al.* [21]. Our estimates indicate an average coating ratio of 48.8%, with a negative IgA index for *Bifidobacteriaceae*, slightly positive IgA indexes for *Bacteroidaceae* and *Clostridiales*, and a positive IgA index for *Enterobacteriaceae* (Fig. 2F).

Relative abundance estimates for periods of inactivity (neonatal, early postnatal) or stability (after 2 years) of the endogenous immune system demonstrate the performance of our model fitting procedure (Fig. 2G). Furthermore, out-of-sample data corresponding to the period of maturation—not used for parameter inference (Fig. 2G, gray area)—was also accurately predicted by the model. This alignment provides indirect support of the underlying assumptions regarding the immune response's impact on microbial community dynamics, lending credibility to the model estimates of the gut lumen (Fig. 2H) for which direct data is unavailable (Fig. 1A).

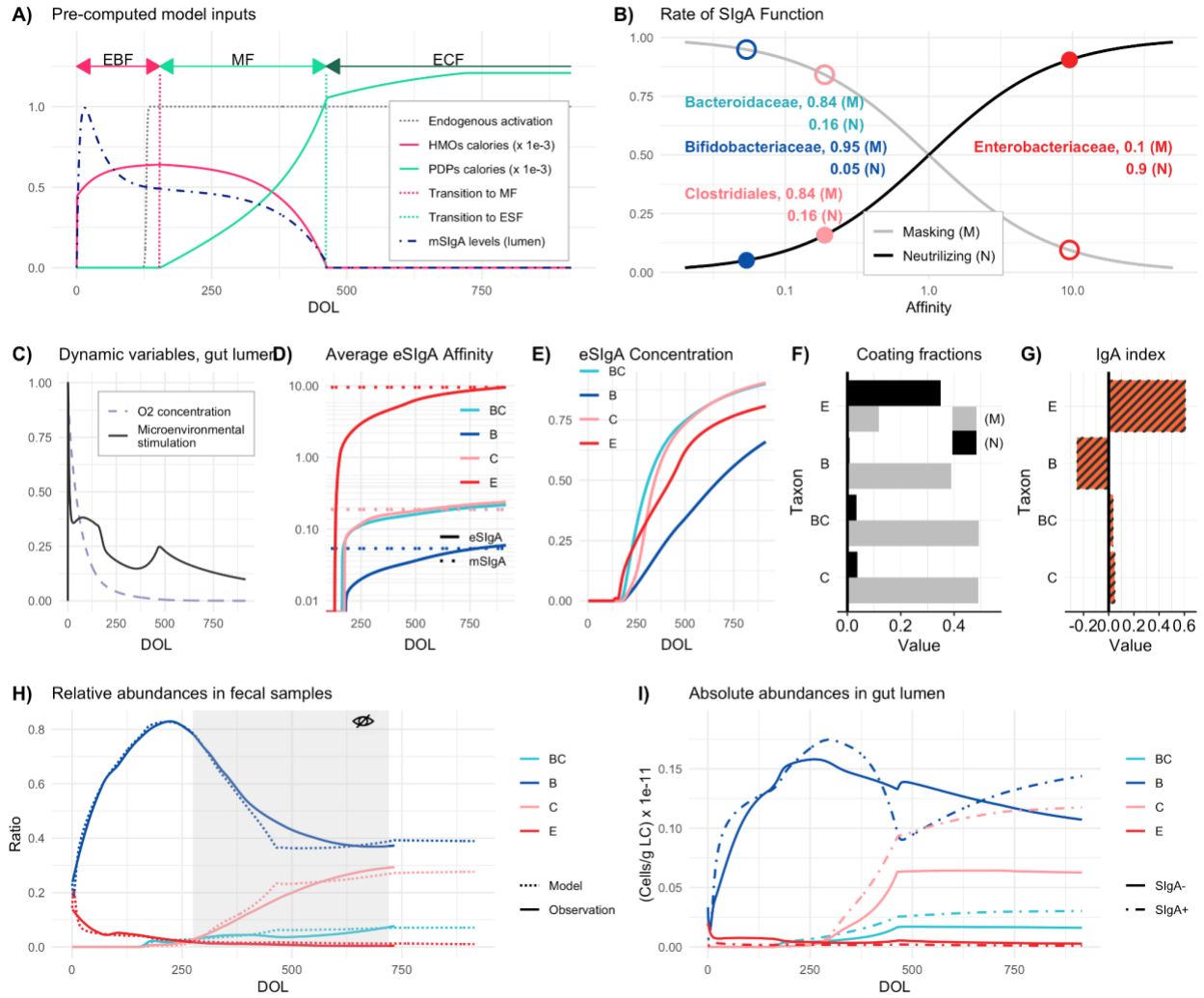

Fig 2. Illustration of Core Mechanisms and Model Fit. (**A**) Model inputs including normalized maternal secretory immunoglobulin A (mSIgA) concentration, human milk oligosaccharide (HMOs) and plant-derived polysaccharides (PDPs) caloric inputs, and timing of the endogenous immune system activation over time, noting that the duration of the different forms of feeding can be altered. EBM: exclusive breastfeeding; MF: mixed feeding; ECF: exclusive complementary feeding. (**B**) Rates and types of SIgA function relative to the level of antibody affinity, where mSIgA values for different taxa are highlighted. Filled and unfilled circles represent the rates of neutralizing and masking, respectively. (**C**) Normalized oxygen concentration and microenvironmental stimulation (normalized by its peak value, reflecting the inflammatory tone of the environment) over time. (**D**) Temporal progression of average endogenous SIgA (eSIgA) affinities (solid lines) gradually approaching the mSIgA affinities (dashed lines), (**E**) and the normalized antibody concentrations in the gut lumen for each key taxon. (**F**) Fractions of masked (M) and neutralized (N) bacteria and (**G**) IgA indexes for each taxon at DOL 735. (**H**) Relative abundances in fecal samples aligned with observational data, where the gray area highlights the out-of-sample data during parameter inference. (**I**) Absolute abundances in the gut lumen for key taxa distinguished by coating status. Model fit estimates for all parameters with their respective description, unit, and prior distribution are provided in Table S3. DOL: Day of life; E:

Enterobacteriaceae; B: *Bifidobacteriaceae*; BC: *Bacteroidaceae*; C: *Clostridiales*; (M): Masking; (N): Neutralizing.

Relative abundance estimates aligned with data points are depicted in Fig. S1, and additional assumptions implicit to the model structure are provided in Table S3. A shiny app is available, to allow exploration of model parameters and emergent phenomena.

IgA-bound Enterobacteriaceae abundance can predict immune phenotypes but only at specific ontogenetic phases

Our ability to develop effective intervention strategies for preventing pathological imprinting hinges on our capacity to accurately predict the trajectory of 'immune education' as the infant gut matures. While there are studies correlating the time course of microbiome composition and IgA-binding patterns with eventual disease susceptibility [59–61], the predictive potential of such analyses at different stages of ontogeny remains underexplored. To evaluate the potential of using taxonomic and IgA-seq profiles of fecal samples to predict the trajectory of infant's immune maturation, we systematically explored variation in ecological and immunological outcomes by simulating our model for a total duration of 735 days across a comprehensive range of exclusive breastfeeding (EBF) and mixed feeding (MF) durations. Across 75.2% of all feeding scenarios, the host's gut mucosal immune response matured to a tolerant profile by simultaneously developing predominantly masking SIgA (rate of masking being above 0.5, higher than rate of neutralizing) against all symbiotic commensals (*Bifidobacteriaceae*, *Bacteroidaceae*; and *Clostridiales*) (Fig. 3A), although the underlying rate of masking varied (Fig. 3B). The infant immune response diverges to a hyperreactive profile—developing predominantly neutralizing antibodies against at least one of the symbiotic commensals across 24.8% of all possible feeding scenarios (Fig. 3A). These results suggest robust convergence towards a tolerogenic profile across a wide spectrum of feeding patterns, in line with previously reported stereotypical convergence of the systemic immune response [2].

Using this synthetically generated data, we explored the diagnostic potential of early life fecal microbiome data in predicting emergent immunopathology. Specifically, we analyzed how effectively the total and SIgA-bound *Enterobacteriaceae* abundance from fecal samples collected at various developmental stages could discriminate between individuals who ultimately developed tolerance versus hyperreactivity after 2 years (at DOL 735). We focused on SIgA-bound Enterobacteriaceae as our primary marker based on the evidence that SIgA coating patterns can identify bacteria associated with immune dysregulation and inflammatory conditions [43]. We first compared the total and SIgA-bound *Enterobacteriaceae* abundance between tolerant and hyperreactive subjects at different time points throughout development. Higher levels of SIgA-bound *Enterobacteriaceae* abundance gradually flip from reflecting tolerant to reflecting hyperreactive immunological states over the time course of ontogeny (Fig. 3D). Lower SIgA-bound *Enterobacteriaceae* observed for hyperreactive phenotypes during early phases of ontogeny are indicative of insufficient *Enterobacteriaceae* neutralization by maternal antibodies. As the host matures, this pattern alters, with the hyperreactive phenotype exhibiting an increase in SIgA-bound *Enterobacteriaceae* abundance relative to the tolerant state, echoing the enrichment in SIgA-coated *Enterobacteriaceae* in adults with IBD-like phenotypes [62,63].

Building on these associations, we next asked how well total and SIgA-bound *Enterobacteriaceae* abundances at different stages of ontogeny could predict immunological phenotypes. We implemented a 5-fold cross-validation approach with stratified sampling to account for potential class imbalances in our binary outcome. For each time point, we fitted three logistic regression models including as covariates: i) total *Enterobacteriaceae* abundance, ii) SIgA-bound *Enterobacteriaceae* abundance, and iii) both total and SIgA-bound *Enterobacteriaceae* abundances. To assess and compare the predictive performance of each model, we calculated the area under the receiver operating characteristic curve (AUC) along with standard errors at each time point. This metric quantifies how well each model discriminates between the two outcome categories, with higher AUC values indicating better classification ability.

Total *Enterobacteriaceae* abundances had the lowest predictive capacity during the first 6 months of life (Fig. 3C, 2E), which can be explained by considering the two compensatory mechanisms regulating it: *i)* ecological competition preventing pathogen overgrowth and *ii)* early activation of the endogenous immune system (earliest at DOL 30) when maternal antibodies are not sufficiently neutralizing. In contrast, SIgA-bound *Enterobacteriaceae* abundance alone during the very early days of life provides valuable information regarding the immunological trajectory (Fig. 3D, 3E), as this quantity reflects the efficiency and/or presence of maternal antibodies [60]. Starting from month 6 (DOL 180), the predictive power of total *Enterobacteriaceae* abundance increases while that of SIgA-bound *Enterobacteriaceae* decreases. This shift indicates that endogenous immune responses against symbiotic commensals combined with ecological competition become the primary regulators of *Enterobacteriaceae* population, exerting stronger selection pressure than the endogenous SIgA response to *Enterobacteriaceae* itself (Fig S2). This shift in predictive powers also coincides with the transition from maternal to endogenous antibody responses. Notably, SIgA-bound *Enterobacteriaceae* samples collected during this transitional period from maternal to endogenous SIgA dominance in the gut lumen provided the least information about the host's immunological trajectory, revealing non-monotonic temporal patterns in the predictive value of 16S rRNA and IgA-seq analyses. Comparison with an independent dataset provided in [64] showed that our model captured similar patterns in the relative importance of microbial and inflammatory predictors (Fig. S11), providing additional support to the plausibility of our results.

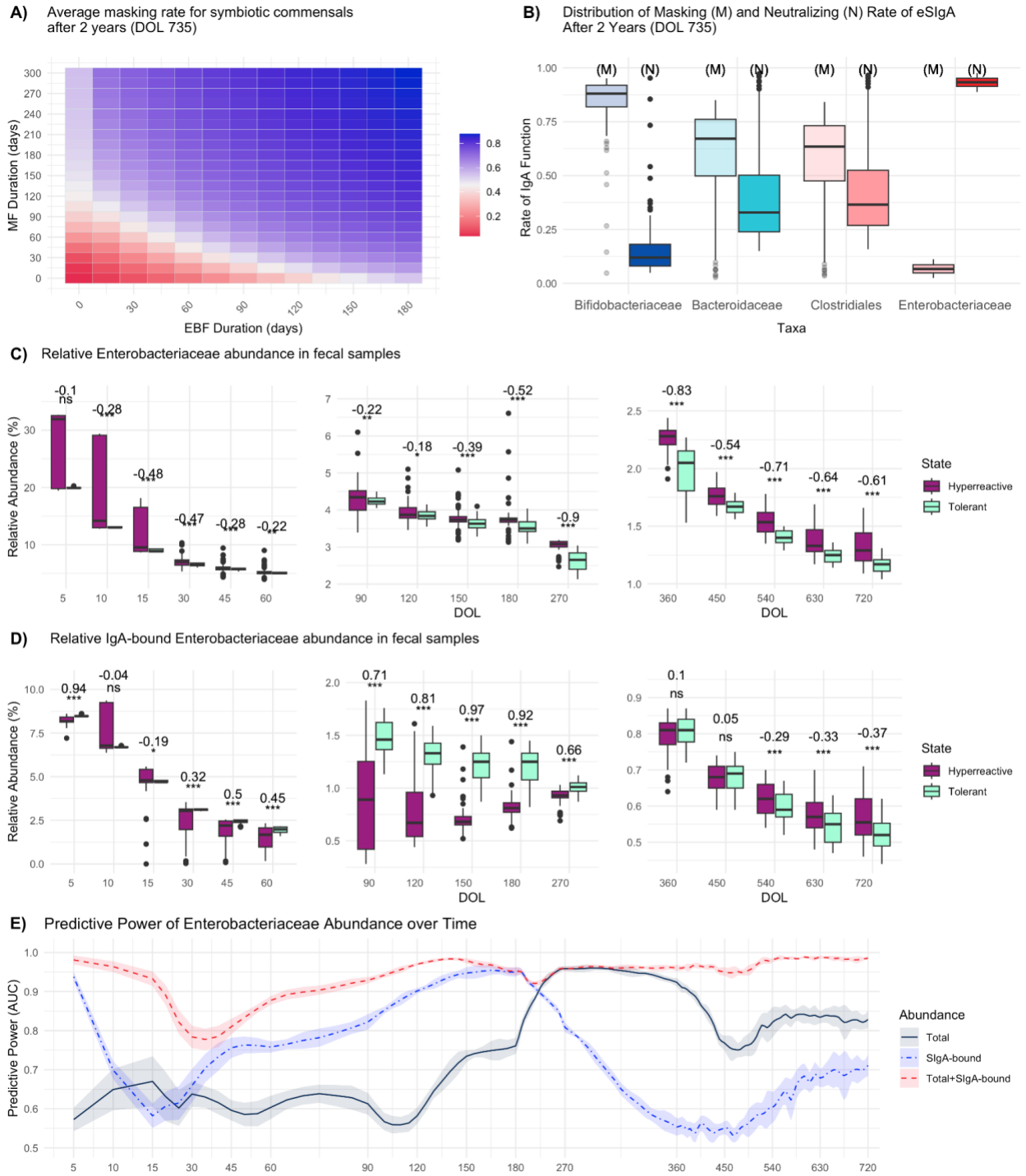

Fig 3. Immunological outcomes and *Enterobacteriaceae* abundances for the first 2 years of life for different combinations of exclusive breastfeeding (EBF) and mixed feeding (MF) durations. (**A**) Immune functionality across a spectrum of EBF and MF durations, where 'tolerant' corresponds to developing predominantly non-neutralizing but masking antibodies against all symbiotic commensals; and 'hyperreactive' otherwise. EBF and MF durations vary from 0 to 180 and to 300 days respectively (**B**) Distribution of masking (M) and neutralizing (N) rates of endogenous SIgA at DOL 735. Distribution of (**C**) total and (**D**) SIgA-bound *Enterobacteriaceae*

abundances over the first two years of life segregated by tolerant (predominantly masking SIgA for all symbiotic commensals simultaneously) and hyperreactive (predominantly neutralizing SIgA for at least one of the symbiotic commensals) states. The dataset is balanced for each time point to reflect the typical sample size of recent cohort studies [65]. A Wilcoxon rank-sum test is used to calculate the effect size (rank-biserial correlation from -1 to +1; values closer to ±1 indicating stronger associations) and the significance (*** for $p < 0.001$, ** for $p < 0.01$, * for $p < 0.05$, . for $p < 0.1$, and ns for $p \geq 0.1$), displayed at the top of each boxplot. (**E**) Mean predictive power (AUC) of *Enterobacteriaceae* abundance segregated by data types. Predictive power of 0.5 indicates no better prediction of a tolerogenic/hyperreactive phenotype than random chance; 1 indicates perfect accuracy. Shaded areas represent ±1 standard error around the mean values. Values are smoothed using a local polynomial regression (LOESS) model. DOL: Day of life; AUC: Area under the receiver operating characteristic curve.

Ecology versus the microenvironment: what carries the information?

An enduring mystery in mucosal immunology is how postnatal influences on the immune system persist into adulthood, even though many core cell types are not present when these initial influences occur [11]. One way to test whether this persistent influence is also reflected in our model is to investigate the impact of EBF duration on affinity maturation: antigenic sampling is delayed if M cells remain immature as a result of persistently high levels of mSIgA, and this postpones the activation of B and T cells until the end of this period. Thus, we expect the influence of the EBF period – if any – to rapidly fade unless other components of the system have enduring effects, since mSIgA has a strict half-life and the delivery of HMOs ceases instantaneously with the cessation of breastfeeding (Fig. S3A).

We first investigate the differential impacts of EBF and MF durations in determining endogenous SIgA (eSIgA) affinity across a comprehensive range of EBF and MF durations. Given the presence of pre-weaning commensals (*Bifidobacteriaceae*, *Enterobacteriaceae*) in the gut lumen during both EBF and MF, eSIgA affinity maturation towards these taxa will be influenced by the duration of both feeding practices. Conversely, a significant role for EBF duration in the affinity maturation against post-weaning commensals (*Bacteroidaceae*, *Clostridiales*) would align with the persistent postnatal influences described above. As hypothesized, immune responses against pre-weaning and post-weaning commensals are impacted by EBF and MF durations differently shown by a predictor importance analysis (Fig 4A), where we compare the relative importance of EBF and MF durations in explaining the variance in eSIgA affinities. Recapitulating the presented conundrum, the influence of EBF duration remains prominent in explaining the variance in eSIgA affinities against post-weaning commensals, despite MF duration being 1.5 times more influential. This influence is more prominent when EBF is followed by Exclusive Complementary Feeding (ECF) without any intervening MF period, which makes it challenging for the host to develop tolerance against post-weaning commensals (Fig. S3B).

Although mSIgA itself may not persist, its initial modifications may continue to shape both the ecology and the inflammatory tone of the microenvironment; similarly, HMOs may have shaped the ecology by selecting for bacteria based on their metabolic capacity, leading to a sustained temporal influence. Therefore, we compare the impact of pre-weaning commensal abundance and the microenvironmental stimulation on eSIgA affinities for post-weaning commensals to identify

which components of our system carry information from the EBF period onward. We employed the Random Forests method to handle correlation between microbial abundances and microenvironmental stimulation. Intriguingly, our findings reveal a significantly greater influence of the microenvironmental stimulation over taxonomic composition (Fig. 4B). These findings suggest that the conditions and signals within the gut microenvironment—such as epithelial permeability and the tolerogenic bias of follicular T cells which are directly modulated by the microenvironmental stimulation in our model—play a pivotal role in shaping the infant's immune response relative to the presence or abundance of specific bacterial taxa. Moreover, these results indicate that breastfeeding's influence extends beyond immediate transmission of HMOs, antibodies, and microbes, conditioning the gut microenvironment in ways that produce effects outlasting the transient presence of such factors. While inflammatory tone and immune maturation undoubtedly have bidirectional interactions in our model making causality difficult to disentangle, our analysis provides evidence for directionality through temporal precedence: early microenvironmental conditions at the start of weaning predict subsequent immune responses against taxa that only appear post-weaning. This temporal sequence helps untangle the cyclic relationship and supports the directionality from early inflammatory tone to downstream immune maturation.

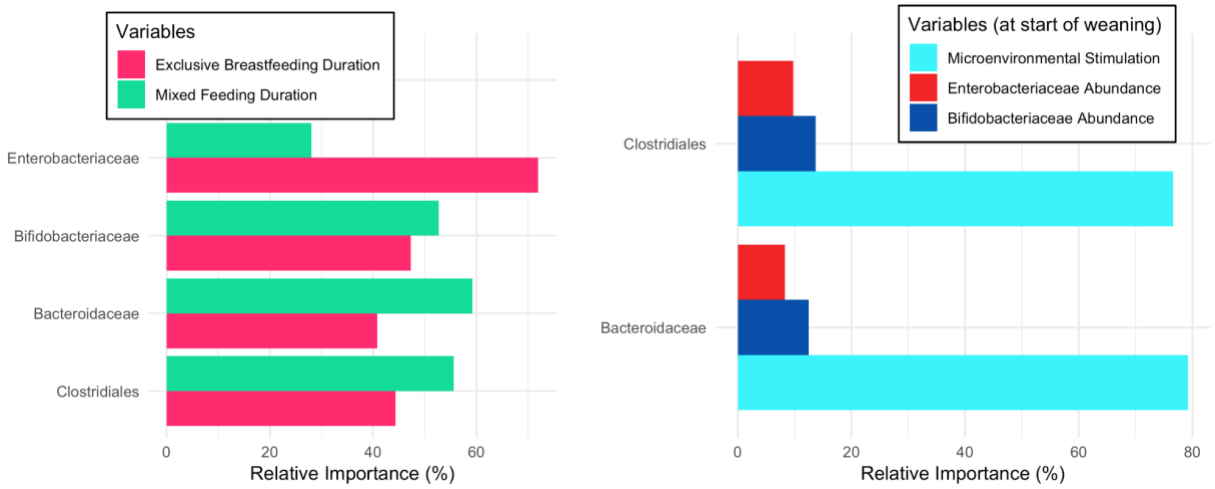

Fig 4. Impact of different feeding durations and environmental variables in determining the matured eSIgA values for key taxa. (**A**) Relative importance analysis in determining the eSIgA values for key taxa, comparing the impact of EBF and MF durations. (**B**) Relative importance analysis in determining the eSIgA values for post-weaning commensals, comparing the impact of the abundances of pre-weaning commensals and the microenvironmental stimulation.

Maternal protection and immunological imprinting in the offspring depends on mother's immunological profile

Despite the well-established health benefits of breastfeeding, it presents a complex decision-making process for mothers experiencing immune dysregulation [66]. While epigenetic regulation of various immune cells, including dendritic cells, stromal cells, T cells, alveolar macrophages, and epithelial cells, has been implicated in the persistence of transgenerational immune priming [12,59], other mechanisms may also play a role. By meticulously eliminating other possibilities such as genetic and epigenetic factors, microbiota variation, and differences in milk-derived

438 metabolites, recent work by Ramanan *et al.* demonstrated that the primary maternal factor allowing
439 for transgenerational immune priming in mice is vertical transmission of maternal IgA [11]. This
440 observation opens up the possibility of transmission of inflammatory phenotypes via maternal IgA,
441 as well as tolerogenic ones. Indeed, evidence suggests that Inflammatory Bowel Disease (IBD) is
442 significantly more prevalent in the offspring of IBD mothers, who tend to produce breastmilk with
443 higher inflammatory potential and lower antibody levels [67–69]; and inadequate levels of
444 maternal SIgA to food allergens have been linked to infantile allergic diseases in breastfed infants,
445 showing a stronger correlation with symptoms than parental atopic history [70]. However,
446 breastmilk's influence goes beyond immune priming and antibody transfer, also enhancing
447 colonization resistance against pathogens through nutritional and microbial support. Therefore, it
448 is not immediately apparent under what circumstances the benefits of breastfeeding outweigh its
449 risk of inflammatory priming.
450
451 To address this question, we compare five different feeding scenarios with varying maternal
452 immunological profiles : *i)* control group recapitulating the scenario in Fig. 2, *ii)* excessive
453 targeting of commensal bacteria by maternal antibodies (high affinity mSIgA against
454 *Bifidobacteriaceae*, *Bacteroidaceae*, and *Clostridiales*), mimicking an IBD-like phenotype [71],
455 *iii)* breastmilk devoid of mIgA but supplying HMOs and *Bifidobacteriaceae*, indicative of a
456 maternal SIgA deficiency, *iv)* exclusive complementary feeding (ECF), with *Bifidobacteriaceae*
457 introduced at a lower inoculum size and delayed introduction of post-weaning taxa
458 (*Bacteroidaceae* and *Clostridiales*), mimicking a scenario with no breastfeeding, and *v)* ECF with
459 *Bacteroidaceae* and *Clostridiales* transfer from the start, mimicking additional probiotic
460 supplementation. In all scenarios, *Enterobacteriaceae* are introduced at the same inoculum size to
461 assess the balance between pathogenic and symbiotic commensals (*Bifidobacteriaceae*,
462 *Bacteroidaceae*, and *Clostridiales*) during the first 30 days of life, a critical period when the infant
463 is particularly vulnerable to pathogen overgrowth.
464
465 Scenarios differed in degree of pathogen control, demonstrating two opposite trends (Fig. 5). ECF
466 with probiotic supplementation (Fig. 5A, 5C; dashed dark purple line) and SIgA-deficient
467 breastfeeding (Fig. 5A, 5C; dashed yellow line) initially showed an increase in the pathogenic-to-
468 symbiotic commensal ratio followed by a decrease that brought them to a similar level by day 10,
469 echoing their similarity in leading to Necrotizing enterocolitis (NEC) [60] and sepsis susceptibility
470 [72]. SIgA-deficient breastfeeding had an initial advantage suggesting that HMOs and
471 *Bifidobacteriaceae* can partially compensate for the lack of mSIgA by directly modulating the gut
472 microbiome composition and thus the colonization resistance against *Enterobacteriaceae*. In
473 contrast, ECF without probiotic supplementation (Fig. 5A, 5C; light green line) resulted in the
474 highest pathogenic-to-symbiotic commensal ratio across all scenarios, emphasizing the importance
475 of key symbiotic commensals in providing defense against pathogens. Interestingly, the second
476 worst outcome in terms of pathogen control was observed with the IBD-like phenotype (Fig. 5
477 dotted magenta line), even though it provides neutralizing antibodies against the pathogenic
478 commensal *Enterobacteriaceae*. The transfer of hyperreactive mSIgA against symbiotic
479 commensals allowed for excessive *Enterobacteriaceae* overgrowth by neutralizing
480 *Bifidobacteriaceae*, leading to significantly higher relative abundances of SIgA-bound
481 *Enterobacteriaceae* in the fecal samples compared to the control group (Fig. 5B).
482

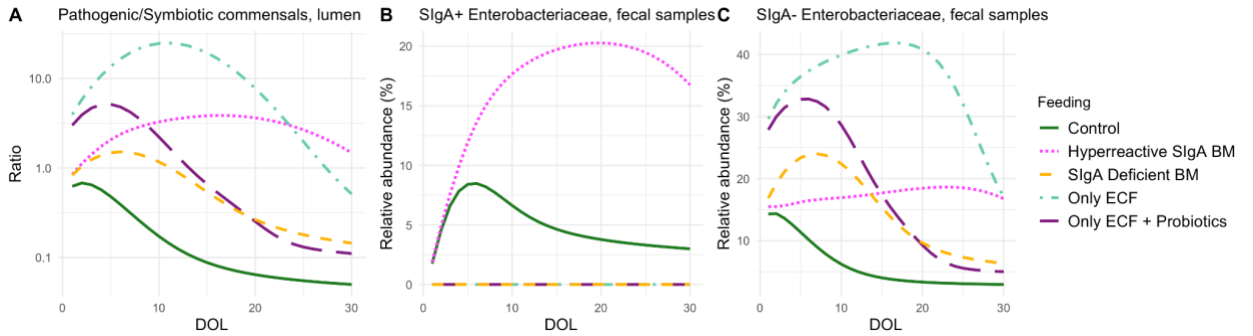

Fig 5. Comparison of various breastfeeding scenarios and their impact on *Enterobacteriaceae* growth. Temporal progression of (**A**) Pathogenic-to-symbiotic commensal ratio in the gut lumen, (**B**) relative SIgA-bound (SIgA+) *Enterobacteriaceae* abundance in fecal samples, and (**C**) relative SIgA-free (SIgA-) *Enterobacteriaceae* abundance in fecal samples of the infant for the first 30 days of life (DOL) for four different breastfeeding scenarios : Control, breastmilk (BM) with hyperreactive mSIgA, mSIgA deficient BM, and only exclusive complementary feeding (ECF).

In all scenarios where breastmilk lacked mSIgA, we observed hyperreactive eSIgA maturation in the infant, highlighting the influence of breastmilk antibody levels in immune imprinting (Table 1, Fig. S4), consistent with findings in the literature [67–70]. In terms of the transgenerational transmission of IgA affinity profiles, our model demonstrates a modulation of hyperreactivity against symbiotic commensals rather than complete transfer of maternal profiles (Table 1, Fig. S4). Offspring hyperreactivity against symbiotic commensals is attenuated relative to maternal hyperreactivity through both antigen-specific and antigen-agnostic mechanisms. In the antigen-specific pathway, the invasiveness of individual bacterial taxa influences offspring developing immune responses, modulated by the limited masking capacity of high-affinity mSIgA in breastmilk (Fig S7). This limited mSIgA masking capacity, combined with the M cells' selective bias for sampling IgA-bacteria complexes [73,74] promotes the accumulation of IgA-coated bacterial antigens in the GALT inductive sites, which activates tolerogenic dendritic cells [75] and dampens the development of high-affinity neutralizing antibodies against symbiotic commensals (Fig 6B, C and D). Simultaneously, an antigen-agnostic pathway operates through microenvironmental stimulation, driven by the cumulative inflammatory capacity of unmasked bacterial subpopulations, with mSIgA's limited masking capacity contributing to a minor reduction in inflammation. Unlike symbiotic commensals, pathogenic bacteria are inherently more invasive, making the mSIgA affinity and the IgA-mediated M cell sampling bias less influential for the taxonomic group *Enterobacteriaceae* in our model (Fig. 6A). The complete transmission of tolerance and the attenuated transmission of hyperreactivity suggest an overall beneficial effect of breastfeeding for developing tolerance against symbiotic commensals, even when the mother has hyperreactive mSIgA in her breastmilk which leads to a suboptimal endogenous antibody development (Table 1, row "Hyperreactive SIgA BM"). This attenuated transmission likely provides a mechanism for gradual normalization of immune responses across generations. However, it is important to note that this result of attenuated transmission of hyperreactivity does not account for potential contributions from maternally derived cytokines (e.g., IL-1β, IL-6, TNF-α, TGF-β) or other mediators transferred through the placenta or breastmilk [76].

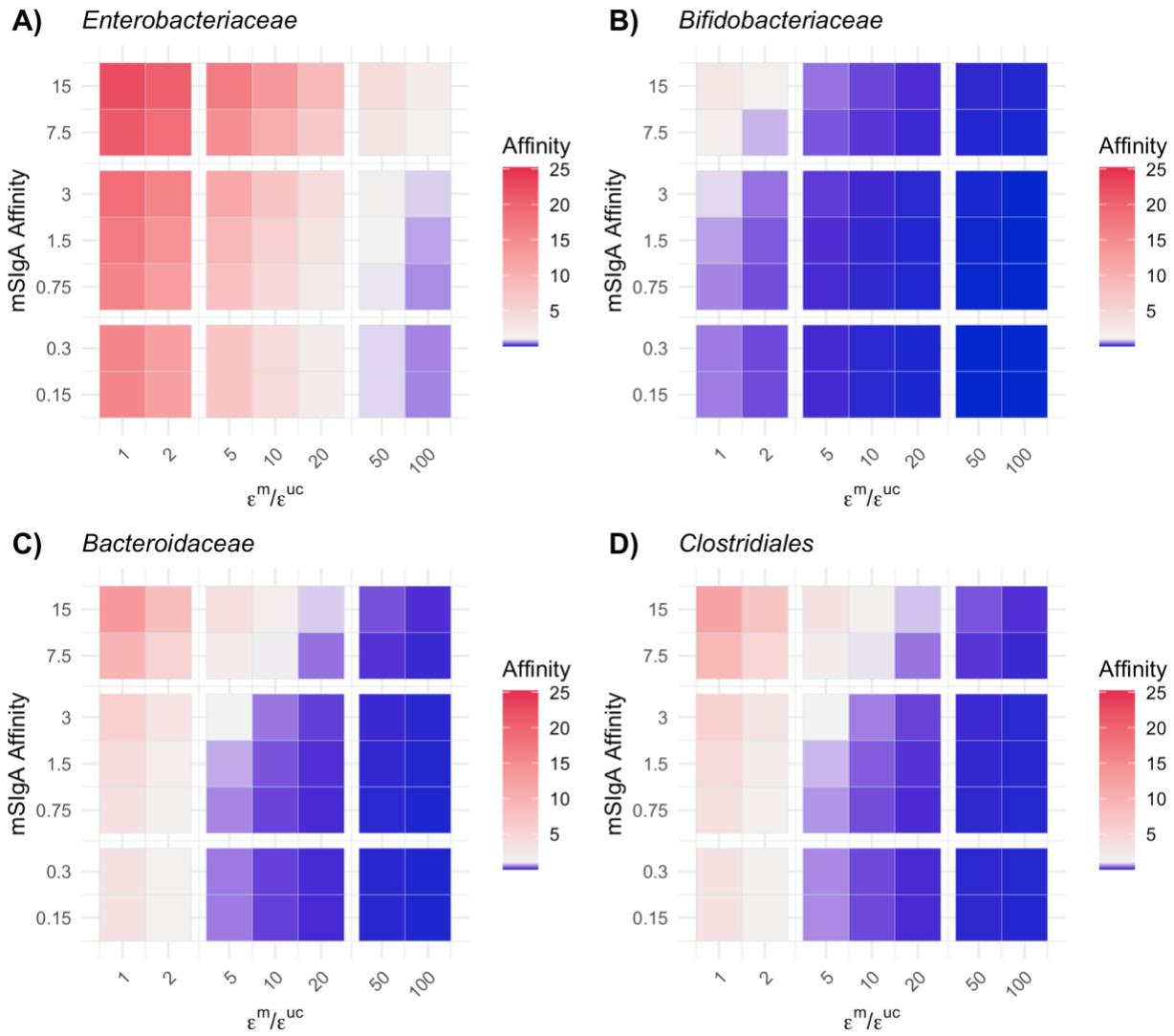

Fig 6. Combined influence of maternal SIgA affinity and antigenic sampling rates on the endogenous SIgA affinities. Heatmaps show endogenous SIgA (eSIgA) affinity levels at two years (DOL 735) across combinations of maternal SIgA (mSIgA) affinities and the ratio of M-cell antigenic sampling rates for masked versus uncoated bacterial antigens (represented by ϵ^m/ϵ^{uc}, where ϵ^m and ϵ^{uc} are the antigenic-sampling rate of masked and uncoated bacterial antigens by M cells, respectively) for **A)** *Enterobacteriaceae*, **B)** *Bifidobacteriaceae*, **C)** *Bacteroidaceae*, and **D)** *Clostridiales*. Color gradients reflect the magnitude of eSIgA affinity: red indicates values greater than 1 (predominantly neutralizing eSIgA), white corresponds to 1, and blue indicates values below 1 (predominantly masking eSIgA).

		Neutralizing (N) rates of SIgA for each taxon			
		Enterobacteriaceae	*Bifidobacteriaceae*	*Bacteroidaceae*	*Clostridiales*
Scenario	**Host**				
Control	Mother	0.90	0.05	0.16	0.16
Control	Offspring	0.89	0.05	0.17	0.18

Hyperreactive SIgA BM	Mother	0.90	0.90	0.90	0.90
Hyperreactive SIgA BM	Offspring	0.92	0.16	0.54	0.53
SIgA Deficient BM	Mother	–	–	–	–
SIgA Deficient BM	Offspring	0.98	0.97	0.97	0.97
Only ECF	Mother	–	–	–	–
Only ECF	Offspring	0.98	0.98	0.96	0.88
Only ECF + Probiotics	Mother	–	–	–	–
Only ECF + Probiotics	Offspring	0.98	0.95	0.97	0.97

Table 1. SIgA profiles in the mother and the offspring for various breastfeeding scenarios. Each column shows the neutralizing (N) rates of SIgA for each taxon, scenario, and host (mother or offspring) combination, as analyzed in Fig. 5. Cell colors indicate the magnitude of the neutralizing (N) rates, with red representing higher values, blue representing lower values, and white indicating zero – aligned with the color scheme in Fig. 6. Note that entries are left blank for scenarios in which the mother either does not breastfeed or has IgA deficiency. Rows for the scenario "Hyperreactive SIgA BM" demonstrate the attenuated transmission of SIgA hyperreactivity from the mother to the offspring. The level of maternal SIgA hyperreactivity is attenuated 82% for *Bifidobacteriaceae* (maternal neutralizing rate of 0.9 translates to a neutralizing rate of 0.16 in the offspring), and 40% for *Bacteroidaceae* and *Clostridiales* (maternal neutralizing rate of 0.9 translates to a neutralizing rates of 0.54 and 0.53 in the offspring, respectively).

Discussion

'Immune education' has proved a powerful concept in understanding the long shadow of early life on health outcomes. Yet, to date, the concept has remained largely qualitative, informally encompassing a wide range of individual components. This diversity and complexity of interactions make integrating these effects by experimental methods alone intractable, quite apart from the question of the degree to which animal models translate to humans. We take the first steps towards formalizing the concept of immune education in the context of gut mucosal SIgA - microbiome interactions, leveraging the power of mathematical frameworks to robustly integrate known feedback loops connecting the ecology and immunology of the gut, and inferring core parameters using data on early life immunity and microbial community dynamics.

Our analysis offers novel qualitative insights that, while grounded in our mechanistic formulations and model assumptions, may inform clinically relevant hypotheses. First, it adds a predictive dimension to the interpretation of gut microbial composition data. Traditional studies, employing 16S rRNA and IgA-seq techniques on fecal samples, have primarily focused on identifying associations between early-life microbiome compositions and later immune-mediated health outcomes. We add mechanistic understanding as to why and how the IgA coating patterns vary over the course of ontogeny by disentangling the influences of maternal and endogenous antibodies. We show that IgA-seq analysis of fecal samples collected during the transitional period—from the gradual decline of maternal antibodies to the rise of endogenous SIgA—has limited predictive value for immunological outcomes. We also reveal opposing temporal trends: reduced SIgA-bound *Enterobacteriaceae* in early ontogeny indicates insufficient maternal

neutralization and predicts hyperreactivity, while the same pattern later suggests tolerogenic imprinting. These non-monotonic temporal patterns suggest that the timing of sample collection critically shapes the ability of 16S rRNA and IgA-seq data to predict long-term immune phenotypes. Moreover, they emphasize the importance of timing in study design and clinical sampling strategies, particularly when sample availability or resources are limited. These findings can be empirically tested through longitudinal studies that assess whether the predictive power of IgA-seq varies systematically across ontogeny, potentially revealing optimal sampling windows for forecasting immune-mediated conditions.

Mixed feeding duration emerges as a critical determinant of the infant's immune trajectory: the sustained presence of maternal antibodies after weaning enables the introduction of novel antigens to the immune system in a non-inflammatory manner, promoting the development of tolerance. Exclusive breastfeeding continues to shape the immune response against microbes introduced even after its cessation by its remnant effects on the inflammatory tone within the gut lumen and GALT inductive sites. This emergent phenomenon suggests a resolution to the perennial question of how information from the early postnatal phase propagates to further stages of immune development: our model indicates that the information is not specifically carried by either symbiotic or pathogenic taxa, but, rather, results from the cumulative capacity of their SIgA-coated and uncoated subpopulations to modulate the inflammatory tone of the microenvironment.

Beyond these fundamental insights, our analysis systematically explores the applied question of how to approach breastfeeding when maternal immunological conditions such as allergies, IBD, or SIgA deficiency affect breastmilk composition. Both lack of SIgA in breastmilk, or excessive targeting of symbiotic commensals by SIgA can lead to suboptimal immune imprinting in the infant, indicating that maternal SIgA is one of the key mechanisms driving the transgenerational transmission of immunological phenotypes. The absence of breastmilk SIgA leads to a fully hyperreactive endogenous SIgA maturation, while hyperreactive maternal SIgA results in an attenuated rather than complete transmission of the inflammatory phenotype. This attenuation occurs through the combination of limited masking by high-affinity maternal SIgA, selective bias of M cells for sampling IgA-bacteria complexes, and the inherently low invasiveness of commensal microbes. Although transfer of *Bifidobacteriaceae* and HMOs cannot entirely compensate for maternal SIgA's role in tolerogenic imprinting, it can partially compensate for the absence of SIgA in pathogen control.

Our findings further provide an evolutionary perspective on the maternal contribution to offspring immune development through breastfeeding. While the absence of breastmilk SIgA leads to significantly impaired immune regulation, our model demonstrates that even "suboptimal" maternal SIgA profiles confer substantial benefits compared to no breastfeeding. This highlights the dual functionality of SIgA: first as an antigen-specific mediator of tolerance, and second as an antigen-agnostic molecule that promotes M cell-mediated antigen sampling [73,74] and programs dendritic cells toward tolerogenic phenotypes [75]. When both functions operate optimally, complete transgenerational transfer of tolerance occurs. However, even when antigen-specific tolerance is impaired (as in maternal inflammatory conditions), the antigen-agnostic properties remain effective, resulting in attenuated rather than complete transmission of maternal hyperreactivity. This mechanism allows for the gradual dilution of inflammatory phenotypes across generations, potentially explaining why some inflammatory conditions do not follow simple

vertical transmission patterns despite breastfeeding. Such a system provides evolutionary resilience, allowing for recovery from dysregulated immune states over generational timescales rather than perpetuating inflammatory phenotypes indefinitely.

These findings, combined with the influence of excess microenvironmental stimulation on endogenous SIgA affinity maturation suggests the possibility of alternative therapeutic approaches for promoting tolerogenic imprinting when maternal immunity is hyperreactive or insufficient. Interventions could focus on strategies to modulate gut inflammation beyond probiotic supplementation, for example targeting Toll-like receptors such as TLR4, which has been proposed to tackle preterm birth and fetal inflammatory injury [77]. Preliminary results from our model indicate the potential effectiveness of this intervention (Fig. S5), suggesting that tolerance could be induced by reducing the inflammatory potential of Gram-negative commensals, similar to the effects observed with TLR4 antagonists. However, a complete exploration of such a scenario would necessitate expanding our model to explicitly incorporate cellular immunity, and to account for the distinct immunological effects of structurally diverse LPS molecules on early-life immune education [78] (Supplementary material, section *Model Limitations*).

Dysregulated immune development in children has repeatedly been shown to mediate multiple pathologies, ranging from developmental deficits in low-resource settings to immune-mediated disorders in developed countries [79]. Given the widespread burden of these conditions, developing a holistic mechanistic understanding of the concept of 'immune education' holds tremendous potential for clinical translation. Therefore, the primary motivation and contribution of this work is to establish the foundations of a mathematical framework for mechanistic thinking, generating clear and testable hypotheses for empirical investigation. Given the immense complexity and dynamism of early life, our model is necessarily a simplification, tailored to the range of data currently available, and excluding factors such as innate immune mechanisms, changes in gut permeability, and strain-specific shifts in the gut microbiome. Although quantitative predictions may change, qualitative conclusions are likely to be robust to these features(Supplementary material, section *Model Limitations*). While we included an illustrative validation using an external dataset (Supplementary Materials, section *Illustrative validation using an external dataset*), this serves primarily as a proof of concept. Future clinical, experimental, and measurement approaches are likely to open the way to evaluating our underlying mechanistic assumptions (Supplementary materials, section *Experimental Model Validation*). Ultimately, our quantitative analysis offers theoretical insights into pressing questions in the field, identifies the gaps in data collection needed to advance mechanistic understanding, and provides a systematic starting point for future data-driven mathematical models of early-life immune development.

647 **References and Notes:**

648 1. Bach J-F. The effect of infections on susceptibility to autoimmune and allergic diseases. N Engl J
649 Med. 2002;347: 911–920. doi:10.1056/nejmra020100

650 2. Olin A, Henckel E, Chen Y, Lakshmikanth T, Pou C, Mikes J, et al. Stereotypic Immune System
651 Development in Newborn Children. Cell. 2018;174: 1277-1292.e14.
652 doi:10.1016/j.cell.2018.06.045

653 3. Steininger H, Moltzau-Anderson J, Lynch SV. Contributions of the early-life microbiome to
654 childhood atopy and asthma development. Semin Immunol. 2023;69: 101795.
655 doi:10.1016/j.smim.2023.101795

656 4. Laforest-Lapointe I, Arrieta M-C. Patterns of Early-Life Gut Microbial Colonization during
657 Human Immune Development: An Ecological Perspective. Front Immunol. 2017;8.
658 doi:10.3389/fimmu.2017.00788

659 5. Hall L. Faculty Opinions recommendation of Temporal development of the gut microbiome in
660 early childhood from the TEDDY study. Fac Opin – Post-Publ Peer Rev Biomed Lit. 2020 [cited
661 12 Apr 2024]. doi:10.3410/f.734278907.793574624

662 6. Zhang L, Agrawal M, Ng SC, Jess T. Early-life exposures and the microbiome: implications for
663 IBD prevention. Gut. 2023; gutjnl-2023-330002. doi:10.1136/gutjnl-2023-330002

664 7. Knoop KA, Gustafsson JK, McDonald KG, Kulkarni DH, Coughlin PE, McCrate S, et al.
665 Microbial antigen encounter during a preweaning interval is critical for tolerance to gut bacteria.
666 Sci Immunol. 2017;2. doi:10.1126/sciimmunol.aao1314

667 8. Belkaid Y, Hand TW. Role of the Microbiota in Immunity and Inflammation. Cell. 2014;157:
668 121–141. doi:10.1016/j.cell.2014.03.011

669 9. Gensollen T, Iyer SS, Kasper DL, Blumberg RS. How colonization by microbiota in early life
670 shapes the immune system. Science. 2016;352: 539–544. doi:10.1126/science.aad9378

671 10. Al Nabhani Z, Dulauroy S, Marques R, Cousu C, Al Bounny S, Déjardin F, et al. A Weaning
672 Reaction to Microbiota Is Required for Resistance to Immunopathologies in the Adult. Immunity.
673 2019;50: 1276-1288.e5. doi:10.1016/j.immuni.2019.02.014

674 11. Ramanan D, Sefik E, Galván-Peña S, Wu M, Yang L, Yang Z, et al. An Immunologic Mode of
675 Multigenerational Transmission Governs a Gut Treg Setpoint. Cell. 2020;181: 1276-1290.e13.
676 doi:10.1016/j.cell.2020.04.030

677 12. Fernandes KA, Lim AI. Maternal-driven immune education in offspring. Immunol Rev. 2024
678 [cited 12 Apr 2024]. doi:10.1111/imr.13315

679 13. Al Nabhani Z, Eberl G. Imprinting of the immune system by the microbiota early in life. Mucosal
680 Immunol. 2020;13: 183–189. doi:10.1038/s41385-020-0257-y

681 14. Torow N, Hand TW, Hornef MW. Programmed and environmental determinants driving neonatal
682 mucosal immune development. Immunity. 2023;56: 485–499. doi:10.1016/j.immuni.2023.02.013

683 15. Wei M, Shinkura R, Doi Y, Maruya M, Fagarasan S, Honjo T. Mice carrying a knock-in mutation

684 of Aicda resulting in a defect in somatic hypermutation have impaired gut homeostasis and
685 compromised mucosal defense. Nat Immunol. 2011;12: 264–270.

686 16. Michaud E, Waeckel L, Gayet R, Goguyer-Deschaumes R, Chanut B, Jospin F, et al. Alteration of
687 microbiota antibody-mediated immune selection contributes to dysbiosis in inflammatory bowel
688 diseases. EMBO Mol Med. 2022;14. doi:10.15252/emmm.202115386

689 17. Pabst O, Slack E. IgA and the intestinal microbiota: the importance of being specific. Mucosal
690 Immunol. 2020;13: 12–21. doi:10.1038/s41385-019-0227-4

691 18. Pabst O, Cerovic V, Hornef M. Secretory IgA in the Coordination of Establishment and
692 Maintenance of the Microbiota. Trends Immunol. 2016;37: 287–296. doi:10.1016/j.it.2016.03.002

693 19. Rogier EW, Frantz AL, Bruno ME, Wedlund L, Cohen DA, Stromberg AJ, et al. Lessons from
694 mother: Long-term impact of antibodies in breast milk on the gut microbiota and intestinal
695 immune system of breastfed offspring. Gut Microbes. 2014;5: 663–668.
696 doi:10.4161/19490976.2014.969984

697 20. Tsukuda N, Yahagi K, Hara T, Watanabe Y, Matsumoto H, Mori H, et al. Key bacterial taxa and
698 metabolic pathways affecting gut short-chain fatty acid profiles in early life. ISME J. 2021;15:
699 2574–2590. doi:10.1038/s41396-021-00937-7

700 21. Planer JD, Peng Y, Kau AL, Blanton LV, Ndao IM, Tarr PI, et al. Development of the gut
701 microbiota and mucosal IgA responses in twins and gnotobiotic mice. Nature. 2016;534: 263–266.
702 doi:10.1038/nature17940

703 22. Pan K. The Effects of Feeding Type on the Gut Microbiota of Neonates and Early Infants. J Infect
704 Dis Case Rep. 2022; 1–5. doi:10.47363/JIDSCR/2022(3)159

705 23. Palmer C, Bik EM, DiGiulio DB, Relman DA, Brown PO. Development of the human infant
706 intestinal microbiota. PLoS Biol. 2007;5: e177.

707 24. Rodríguez JM, Murphy K, Stanton C, Ross RP, Kober OI, Juge N, et al. The composition of the
708 gut microbiota throughout life, with an emphasis on early life. Microb Ecol Health Dis. 2015;26.
709 doi:10.3402/mehd.v26.26050

710 25. Wambach K, Riordan J. Breastfeeding and Human Lactation. Jones & Bartlett Learning; 2016.

711 26. (U.S.) SSNP for W Infants, and Children, (U.S.) CSFP. Infant Nutrition and Feeding: A Guide for
712 Use in the WIC and CSF Programs. United States Department of Agriculture; 2009.

713 27. Mannel R, Martens PJ, Walker M. Core Curriculum for Lactation Consultant Practice. Jones &
714 Bartlett Publishers; 2012.

715 28. Pichler MJ, Yamada C, Shuoker B, Alvarez-Silva C, Gotoh A, Leth ML, et al. Butyrate producing
716 colonic Clostridiales metabolise human milk oligosaccharides and cross feed on mucin via
717 conserved pathways. Nat Commun. 2020;11. doi:10.1038/s41467-020-17075-x

718 29. Wang J, Chen C, Yu Z, He Y, Yong Q, Newburg DS. Relative fermentation of oligosaccharides
719 from human milk and plants by gut microbes. Eur Food Res Technol. 2016;243: 133–146.
720 doi:10.1007/s00217-016-2730-0

721 30. Sela DA. Bifidobacterial utilization of human milk oligosaccharides. Int J Food Microbiol.
722 2011;149: 58–64. doi:10.1016/j.ijfoodmicro.2011.01.025

723 31. Flint HJ, Scott KP, Duncan SH, Louis P, Forano E. Microbial degradation of complex
724 carbohydrates in the gut. Gut Microbes. 2012;3: 289–306. doi:10.4161/gmic.19897

725 32. Marcobal A, Barboza M, Froehlich JW, Block DE, German JB, Lebrilla CB, et al. Consumption of
726 Human Milk Oligosaccharides by Gut-Related Microbes. J Agric Food Chem. 2010;58: 5334–
727 5340. doi:10.1021/jf9044205

728 33. Torow N, Li R, Hitch TCA, Mingels C, Al Bounny S, van Best N, et al. M cell maturation and
729 cDC activation determine the onset of adaptive immune priming in the neonatal Peyer's patch.
730 Immunity. 2023;56: 1220-1238.e7. doi:10.1016/j.immuni.2023.04.002

731 34. Mörbe UM, Jørgensen PB, Fenton TM, von Burg N, Riis LB, Spencer J, et al. Human gut-
732 associated lymphoid tissues (GALT); diversity, structure, and function. Mucosal Immunol.
733 2021;14: 793–802. doi:10.1038/s41385-021-00389-4

734 35. Wagner C, Torow N, Hornef MW, Lelouard H. Spatial and temporal key steps in early-life
735 intestinal immune system development and education. FEBS J. 2021;289: 4731–4757.
736 doi:10.1111/febs.16047

737 36. van der Waaij LA, Kroese FG, Visser A, Nelis GF, Westerveld BD, Jansen PL, et al.
738 Immunoglobulin coating of faecal bacteria in inflammatory bowel disease. Eur J Gastroenterol
739 Hepatol. 2004;16: 669–674. doi:10.1097/01.meg.0000108346.41221.19

740 37. Pop M, Walker AW, Paulson J, Lindsay B, Antonio M, Hossain MA, et al. Diarrhea in young
741 children from low-income countries leads to large-scale alterations in intestinal microbiota
742 composition. Genome Biol. 2014;15: 1–12.

743 38. Ley D, Desseyn J-L, Gouyer V, Plet S, Tims S, Renes I, et al. Early life nutrition influences
744 susceptibility to chronic inflammatory colitis in later life. Sci Rep. 2019;9: 18111.

745 39. Wernroth M-L, Peura S, Hedman AM, Hetty S, Vicenzi S, Kennedy B, et al. Development of gut
746 microbiota during the first 2 years of life. Sci Rep. 2022;12: 9080.

747 40. Lakhdari O, Tap J, Béguet-Crespel F, Le Roux K, de Wouters T, Cultrone A, et al. Identification
748 of NF-κB Modulation Capabilities within Human Intestinal Commensal Bacteria. J Biomed
749 Biotechnol. 2011;2011: 1–9. doi:10.1155/2011/282356

750 41. Schirmer M, Smeekens SP, Vlamakis H, Jaeger M, Oosting M, Franzosa EA, et al. Linking the
751 Human Gut Microbiome to Inflammatory Cytokine Production Capacity. Cell. 2016;167: 1897.
752 doi:10.1016/j.cell.2016.11.046

753 42. Peterson LW, Artis D. Intestinal epithelial cells: regulators of barrier function and immune
754 homeostasis. Nat Rev Immunol. 2014;14: 141–153. doi:10.1038/nri3608

755 43. Palm NW, de Zoete MR, Cullen TW, Barry NA, Stefanowski J, Hao L, et al. Immunoglobulin A
756 Coating Identifies Colitogenic Bacteria in Inflammatory Bowel Disease. Cell. 2014;158: 1000–
757 1010. doi:10.1016/j.cell.2014.08.006

758 44. Donald K, Petersen C, Turvey SE, Finlay BB, Azad MB. Secretory IgA: Linking microbes,
759 maternal health, and infant health through human milk. Cell Host Microbe. 2022;30: 650–659.
760 doi:10.1016/j.chom.2022.02.005

761 45. Brandtzaeg P. Mucosal immunity: integration between mother and the breast-fed infant. Vaccine.
762 2003;21: 3382–3388.

763 46. Donaldson GP, Ladinsky MS, Yu KB, Sanders JG, Yoo BB, Chou W-C, et al. Gut microbiota
764 utilize immunoglobulin A for mucosal colonization. Science. 2018;360: 795–800.
765 doi:10.1126/science.aaq0926

766 47. Van Tassell ML, Miller MJ. Lactobacillus Adhesion to Mucus. Nutrients. 2011;3: 613–636.
767 doi:10.3390/nu3050613

768 48. Cerutti A. Location, location, location: B-cell differentiation in the gut lamina propria. Mucosal
769 Immunol. 2008;1: 8–10. doi:10.1038/mi.2007.8

770 49. Bunker JJ, Bendelac A. IgA responses to microbiota. Immunity. 2018;49: 211–224.

771 50. Lycke NY, Bemark M. The role of Peyer's patches in synchronizing gut IgA responses. Front
772 Immunol. 2012;3. doi:10.3389/fimmu.2012.00329

773 51. Artis D. Epithelial-cell recognition of commensal bacteria and maintenance of immune
774 homeostasis in the gut. Nat Rev Immunol. 2008;8: 411–420. doi:10.1038/nri2316

775 52. Bemark M, Angeletti D. Know your enemy or find your friend?—Induction of IgA at mucosal
776 surfaces. Immunol Rev. 2021;303: 83–102.

777 53. Cerutti A, Rescigno M. The biology of intestinal immunoglobulin A responses. Immunity.
778 2008;28: 740–750.

779 54. Cong Y, Feng T, Fujihashi K, Schoeb TR, Elson CO. A dominant, coordinated T regulatory cell-
780 IgA response to the intestinal microbiota. Proc Natl Acad Sci. 2009;106: 19256–19261.

781 55. Ng KW, Hobbs A, Wichmann C, Victora GD, Donaldson GP. B cell responses to the gut
782 microbiota. Advances in Immunology. Elsevier; 2022. pp. 95–131. doi:10.1016/bs.ai.2022.08.003

783 56. Pietrzak B, Tomela K, Olejnik-Schmidt A, Mackiewicz A, Schmidt M. Secretory IgA in intestinal
784 mucosal secretions as an adaptive barrier against microbial cells. Int J Mol Sci. 2020;21: 9254.

785 57. Senn V, Bassler D, Choudhury R, Scholkmann F, Righini-Grunder F, Vuille-dit-Bille RN, et al.
786 Microbial Colonization From the Fetus to Early Childhood—A Comprehensive Review. Front
787 Cell Infect Microbiol. 2020;10. doi:10.3389/fcimb.2020.573735

788 58. Tang Q, Jin G, Wang G, Liu T, Liu X, Wang B, et al. Current Sampling Methods for Gut
789 Microbiota: A Call for More Precise Devices. Front Cell Infect Microbiol. 2020;10.
790 doi:10.3389/fcimb.2020.00151

791 59. Sarkar A, Yoo JY, Valeria Ozorio Dutra S, Morgan KH, Groer M. The Association between Early-
792 Life Gut Microbiota and Long-Term Health and Diseases. J Clin Med. 2021;10: 459.
793 doi:10.3390/jcm10030459

794 60. Gopalakrishna KP, Macadangdang BR, Rogers MB, Tometich JT, Firek BA, Baker R, et al.
795 Maternal IgA protects against the development of necrotizing enterocolitis in preterm infants. Nat
796 Med. 2019;25: 1110–1115. doi:10.1038/s41591-019-0480-9

797 61. Kostic AD, Gevers D, Siljander H, Vatanen T, Hyötyläinen T, Hämäläinen A-M, et al. The
798 Dynamics of the Human Infant Gut Microbiome in Development and in Progression toward Type
799 1 Diabetes. Cell Host Microbe. 2015;17: 260–273. doi:10.1016/j.chom.2015.01.001

800 62. Viladomiu M, Kivolowitz C, Abdulhamid A, Dogan B, Victorio D, Castellanos JG, et al. IgA-
801 coated E. coli enriched in Crohn's disease spondyloarthritis promote
802 T H 17-dependent inflammation. Sci Transl Med. 2017;9.
803 doi:10.1126/scitranslmed.aaf9655

804 63. DuPont HL, Jiang Z-D, Alexander AS, DuPont AW, Brown EL. Intestinal IgA-Coated Bacteria in
805 Healthy- and Altered-Microbiomes (Dysbiosis) and Predictive Value in Successful Fecal
806 Microbiota Transplantation. Microorganisms. 2022;11: 93. doi:10.3390/microorganisms11010093

807 64. Olivares M, Walker AW, Capilla A, Benítez-Páez A, Palau F, Parkhill J, et al. Gut microbiota
808 trajectory in early life may predict development of celiac disease. Microbiome. 2018;6: 1–11.

809 65. Stewart CJ, Ajami NJ, O'Brien JL, Hutchinson DS, Smith DP, Wong MC, et al. Temporal
810 development of the gut microbiome in early childhood from the TEDDY study. Nature. 2018;562:
811 583–588. doi:10.1038/s41586-018-0617-x

812 66. Barrett EG. Maternal influence in the transmission of asthma susceptibility. Pulm Pharmacol Ther.
813 2008;21: 474–484. doi:10.1016/j.pupt.2007.06.005

814 67. Dotan I, Alper A, Rachmilewitz D, Israeli E, Odes S, Chermesh I, et al. Maternal inflammatory
815 bowel disease has short and long-term effects on the health of their offspring: A multicenter study
816 in Israel. J Crohns Colitis. 2013;7: 542–550. doi:10.1016/j.crohns.2012.08.012

817 68. Meng X, Dunsmore G, Koleva P, Elloumi Y, Wu RY, Sutton RT, et al. The Profile of Human
818 Milk Metabolome, Cytokines, and Antibodies in Inflammatory Bowel Diseases Versus Healthy
819 Mothers, and Potential Impact on the Newborn. J Crohns Colitis. 2018;13: 431–441.
820 doi:10.1093/ecco-jcc/jjy186

821 69. Torres J, Hu J, Seki A, Eisele C, Nair N, Huang R, et al. Infants born to mothers with IBD present
822 with altered gut microbiome that transfers abnormalities of the adaptive immune system to germ-
823 free mice. Gut. 2019;69: 42–51. doi:10.1136/gutjnl-2018-317855

824 70. MacHtinger S, Moss R. Cow's milk allergy in breast-fed infants: The role of allergen and maternal
825 secretory IgA antibody. J Allergy Clin Immunol. 1986;77: 341–347. doi:10.1016/s0091-
826 6749(86)80115-4

827 71. Russler-Germain EV, Rengarajan S, Hsieh C-S. Antigen-specific regulatory T-cell responses to
828 intestinal microbiota. Mucosal Immunol. 2017;10: 1375–1386. doi:10.1038/mi.2017.65

829 72. Pietrasanta C, Carlosama C, Lizier M, Fornasa G, Jost TR, Carloni S, et al. Prenatal antibiotics
830 reduce breast milk IgA and induce dysbiosis in mouse offspring, increasing neonatal susceptibility
831 to bacterial sepsis. Cell Host Microbe. 2024;32: 2178–2194.

832 73. Mantis NJ, Cheung MC, Chintalacharuvu KR, Rey J, Corthésy B, Neutra MR. Selective adherence
833 of IgA to murine Peyer's patch M cells: evidence for a novel IgA receptor. J Immunol. 2002;169:
834 1844–1851.

835 74. Rol N, Favre L, Benyacoub J, Corthésy B. The role of secretory immunoglobulin A in the natural
836 sensing of commensal bacteria by mouse Peyer's patch dendritic cells. J Biol Chem. 2012;287:
837 40074–40082.

838 75. Diana J, Moura IC, Vaugier C, Gestin A, Tissandie E, Beaudoin L, et al. Secretory IgA induces
839 tolerogenic dendritic cells through SIGNR1 dampening autoimmunity in mice. J Immunol.
840 2013;191: 2335–2343.

841 76. Lim AI, McFadden T, Link VM, Han S-J, Karlsson R-M, Stacy A, et al. Prenatal maternal
842 infection promotes tissue-specific immunity and inflammation in offspring. Science. 2021;373:
843 eabf3002.

844 77. Robertson SA, Hutchinson MR, Rice KC, Chin P, Moldenhauer LM, Stark MJ, et al. Targeting
845 Toll-like receptor-4 to tackle preterm birth and fetal inflammatory injury. Clin Transl Immunol.
846 2020;9. doi:10.1002/cti2.1121

847 78. Vatanen T, Kostic AD, d'Hennezel E, Siljander H, Franzosa EA, Yassour M, et al. Variation in
848 microbiome LPS immunogenicity contributes to autoimmunity in humans. Cell. 2016;165: 842–
849 853.

850 79. Kadia BM, Allen SJ. Effect of pre-, pro-, and synbiotics on biomarkers of systemic inflammation
851 in children: a scoping review. Nutrients. 2024;16: 336.

852 80. Torow N, Hornef MW. The Neonatal Window of Opportunity: Setting the Stage for Life-Long
853 Host-Microbial Interaction and Immune Homeostasis. J Immunol. 2017;198: 557–563.
854 doi:10.4049/jimmunol.1601253

855 81. Bemark M, Pitcher MJ, Dionisi C, Spencer J. Gut-associated lymphoid tissue: a microbiota-driven
856 hub of B cell immunity. Trends Immunol. 2024;45: 211–223. doi:10.1016/j.it.2024.01.006

857 82. Sugahara H, Okai S, Odamaki T, Wong CB, Kato K, Mitsuyama E, et al. Decreased Taxon-
858 Specific IgA Response in Relation to the Changes of Gut Microbiota Composition in the Elderly.
859 Front Microbiol. 2017;8. doi:10.3389/fmicb.2017.01757

860 83. May RM. Stability and Complexity in Model Ecosystems. 2001 [cited 13 Apr 2024].
861 doi:10.1515/9780691206912

862 84. Bucci V, Tzen B, Li N, Simmons M, Tanoue T, Bogart E, et al. MDSINE: Microbial Dynamical
863 Systems INference Engine for microbiome time-series analyses. Genome Biol. 2016;17.
864 doi:10.1186/s13059-016-0980-6

865 85. Stein RR, Bucci V, Toussaint NC, Buffie CG, Rätsch G, Pamer EG, et al. Ecological modeling
866 from time-series inference: insight into dynamics and stability of intestinal microbiota. PLoS
867 Comput Biol. 2013;9: e1003388.

868 86. Marino S, Baxter NT, Huffnagle GB, Petrosino JF, Schloss PD. Mathematical modeling of
869 primary succession of murine intestinal microbiota. Proc Natl Acad Sci. 2014;111: 439–444.

87. Molari M, Eyer K, Baudry J, Cocco S, Monasson R. Quantitative modeling of the effect of antigen dosage on B-cell affinity distributions in maturating germinal centers. Elife. 2020;9: e55678.

88. Thomas MJ, Klein U, Lygeros J, Rodríguez Martínez M. A Probabilistic Model of the Germinal Center Reaction. Front Immunol. 2019;10. doi:10.3389/fimmu.2019.00689

89. Buchauer L, Wardemann H. Calculating germinal centre reactions. Curr Opin Syst Biol. 2019;18: 1–8.

90. Wang S, Mata-Fink J, Kriegsman B, Hanson M, Irvine DJ, Eisen HN, et al. Manipulating the selection forces during affinity maturation to generate cross-reactive HIV antibodies. Cell. 2015;160: 785–797.

91. Koshkin A, Herbach U, Martínez MR, Gandrillon O, Crauste F. Stochastic modeling of a gene regulatory network driving B cell development in germinal centers. Plos One. 2024;19: e0301022.

92. Pélissier A, Akrout Y, Jahn K, Kuipers J, Klein U, Beerenwinkel N, et al. Computational model reveals a stochastic mechanism behind germinal center clonal bursts. Cells. 2020;9: 1448.

93. Merkenschlager J, Pyo AG, Silva Santos GS, Schaefer-Babajew D, Cipolla M, Hartweger H, et al. Regulated somatic hypermutation enhances antibody affinity maturation. Nature. 2025; 1–8.

94. Mikulic J, Longet S, Favre L, Benyacoub J, Corthesy B. Secretory IgA in complex with Lactobacillus rhamnosus potentiates mucosal dendritic cell-mediated Treg cell differentiation via TLR regulatory proteins, RALDH2 and secretion of IL-10 and TGF-β. Cell Mol Immunol. 2016;14: 546–556. doi:10.1038/cmi.2015.110

95. Atyeo C, Alter G. The multifaceted roles of breast milk antibodies. Cell. 2021;184: 1486–1499. doi:10.1016/j.cell.2021.02.031

96. Onyiah JC, Colgan SP. Cytokine responses and epithelial function in the intestinal mucosa. Cell Mol Life Sci. 2016;73: 4203–4212.

97. Turner JR. Intestinal mucosal barrier function in health and disease. Nat Rev Immunol. 2009;9: 799–809. doi:10.1038/nri2653

98. Dillon A, Lo DD. M Cells: Intelligent Engineering of Mucosal Immune Surveillance. Front Immunol. 2019;10. doi:10.3389/fimmu.2019.01499

99. Ohkusa T, Yoshida T, Sato N, Watanabe S, Tajiri H, Okayasu I. Commensal bacteria can enter colonic epithelial cells and induce proinflammatory cytokine secretion: a possible pathogenic mechanism of ulcerative colitis. J Med Microbiol. 2009;58: 535–545. doi:10.1099/jmm.0.005801-0

100. Pabst O. New concepts in the generation and functions of IgA. Nat Rev Immunol. 2012;12: 821–832. doi:10.1038/nri3322

101. Fransen F, Zagato E, Mazzini E, Fosso B, Manzari C, El Aidy S, et al. BALB/c and C57BL/6 Mice Differ in Polyreactive IgA Abundance, which Impacts the Generation of Antigen-Specific IgA and Microbiota Diversity. Immunity. 2015;43: 527–540. doi:10.1016/j.immuni.2015.08.011

906 102. Liu Y, Rhoads J. Communication between B-Cells and Microbiota for the Maintenance of
907 Intestinal Homeostasis. Antibodies. 2013;2: 535–553. doi:10.3390/antib2040535

908 103. Ding M, Yang B, Ross RP, Stanton C, Zhao J, Zhang H, et al. Crosstalk between sIgA-Coated
909 Bacteria in Infant Gut and Early-Life Health. Trends Microbiol. 2021;29: 725–735.
910 doi:10.1016/j.tim.2021.01.012

911 104. Berkowska MA, Schickel J-N, Grosserichter-Wagener C, de Ridder D, Ng YS, van Dongen JJM,
912 et al. Circulating Human CD27−IgA+ Memory B Cells Recognize Bacteria with Polyreactive Igs.
913 J Immunol. 2015;195: 1417–1426. doi:10.4049/jimmunol.1402708

914 105. Iyer K, Erkert L, Becker C. Know your neighbors: microbial recognition at the intestinal barrier
915 and its implications for gut homeostasis and inflammatory bowel disease. Front Cell Dev Biol.
916 2023;11. doi:10.3389/fcell.2023.1228283

917 106. Mahapatro M, Erkert L, Becker C. Cytokine-Mediated Crosstalk between Immune Cells and
918 Epithelial Cells in the Gut. Cells. 2021;10: 111. doi:10.3390/cells10010111

919 107. Goto Y, Kiyono H. Epithelial barrier: an interface for the cross-communication between gut flora
920 and immune system. Immunol Rev. 2011;245: 147–163. doi:10.1111/j.1600-065x.2011.01078.x

921 108. Martin-Gallausiaux C, Marinelli L, Blottière HM, Larraufie P, Lapaque N. SCFA: mechanisms
922 and functional importance in the gut. Proc Nutr Soc. 2020;80: 37–49.
923 doi:10.1017/s0029665120006916

924 109. Li Y, Faden HS, Zhu L. The Response of the Gut Microbiota to Dietary Changes in the First Two
925 Years of Life. Front Pharmacol. 2020;11. doi:10.3389/fphar.2020.00334

926 110. Laursen MF. Gut Microbiota Development: Influence of Diet from Infancy to Toddlerhood. Ann
927 Nutr Metab. 2021;77: 21–34. doi:10.1159/000517912

928 111. Appert O, Garcia AR, Frei R, Roduit C, Constancias F, Neuzil-Bunesova V, et al. Initial butyrate
929 producers during infant gut microbiota development are endospore formers. Environ Microbiol.
930 2020;22: 3909–3921. doi:10.1111/1462-2920.15167

931 112. Hooper LV, Littman DR, Macpherson AJ. Interactions Between the Microbiota and the Immune
932 System. Science. 2012;336: 1268–1273. doi:10.1126/science.1223490

933 113. Zhu J, Paul WE. Peripheral CD4+ T-cell differentiation regulated by networks of cytokines and
934 transcription factors. Immunol Rev. 2010;238: 247–262. doi:10.1111/j.1600-065x.2010.00951.x

935 114. Ma X, Nakayamada S, Wang J. Multi-Source Pathways of T Follicular Helper Cell Differentiation.
936 Front Immunol. 2021;12. doi:10.3389/fimmu.2021.621105

937 115. Reboldi A, Cyster JG. Peyer's patches: organizing B-cell responses at the intestinal frontier.
938 Immunol Rev. 2016;271: 230–245. doi:10.1111/imr.12400

939 116. Kumamoto Y, Hirai T, Wong PW, Kaplan DH, Iwasaki A. CD301b+ dendritic cells suppress T
940 follicular helper cells and antibody responses to protein antigens. eLife. 2016;5.
941 doi:10.7554/elife.17979

942 117. Ko H-J, Chang S-Y. Regulation of Intestinal Immune System by Dendritic Cells. Immune Netw.
943 2015;15: 1. doi:10.4110/in.2015.15.1.1

944 118. Favre L, Spertini F, Corthésy B. Secretory IgA Possesses Intrinsic Modulatory Properties
945 Stimulating Mucosal and Systemic Immune Responses. J Immunol. 2005;175: 2793–2800.
946 doi:10.4049/jimmunol.175.5.2793

947 119. Morbach H, Eichhorn EM, Liese JG, Girschick HJ. Reference values for B cell subpopulations
948 from infancy to adulthood. Clin Exp Immunol. 2010;162: 271–279. doi:10.1111/j.1365-
949 2249.2010.04206.x

950 120. Cashman KS, Jenks SA, Woodruff MC, Tomar D, Tipton CM, Scharer CD, et al. Understanding
951 and measuring human B-cell tolerance and its breakdown in autoimmune disease. Immunol Rev.
952 2019;292: 76–89. doi:10.1111/imr.12820

953 121. Davis CL, Wahid R, Toapanta FR, Simon JK, Sztein MB, Levy D. Applying Mathematical Tools
954 to Accelerate Vaccine Development: Modeling Shigella Immune Dynamics. PLoS ONE. 2013;8:
955 e59465. doi:10.1371/journal.pone.0059465

956 122. Tellier J, Nutt SL. The secret to longevity, plasma cell style. Nat Immunol. 2022;23: 1507–1508.
957 doi:10.1038/s41590-022-01340-w

958 123. Siegrist C-A, Aspinall R. B-cell responses to vaccination at the extremes of age. Nat Rev
959 Immunol. 2009;9: 185–194. doi:10.1038/nri2508

960 124. Semmes EC, Chen J-L, Goswami R, Burt TD, Permar SR, Fouda GG. Understanding Early-Life
961 Adaptive Immunity to Guide Interventions for Pediatric Health. Front Immunol. 2021;11.
962 doi:10.3389/fimmu.2020.595297

963 125. Gustafson CE, Higbee D, Yeckes AR, Wilson CC, De Zoeten EF, Jedlicka P, et al. Limited
964 expression of APRIL and its receptors prior to intestinal IgA plasma cell development during
965 human infancy. Mucosal Immunol. 2014;7: 467–477. doi:10.1038/mi.2013.64

966 126. Stan Development Team. (2020). RStan: the R interface to Stan. http://mc-stan.org/.

967 127. Bishop CM. Pattern Recognition and Machine Learning. Springer; 2016.

968 128. Damaceno QS, Souza JP, Nicoli JR, Paula RL, Assis GB, Figueiredo HC, et al. Evaluation of
969 Potential Probiotics Isolated from Human Milk and Colostrum. Probiotics Antimicrob Proteins.
970 2017;9: 371–379. doi:10.1007/s12602-017-9270-1

971 129. Chia LW, Mank M, Blijenberg B, Bongers RS, van Limpt K, Wopereis H, et al. Cross-feeding
972 between Bifidobacterium infantis and Anaerostipes caccae on lactose and human milk
973 oligosaccharides. Benef Microbes. 2021;12: 69–83. doi:10.3920/bm2020.0005

974 130. Vidanaarachchi R, Shaw M, Tang S-L, Halgamuge S. IMPARO: inferring microbial interactions
975 through parameter optimisation. BMC Mol Cell Biol. 2020;21. doi:10.1186/s12860-020-00269-y

976 131. Huang Y, Sheth RU, Zhao S, Cohen LA, Dabaghi K, Moody T, et al. High-throughput microbial
977 culturomics using automation and machine learning. Nat Biotechnol. 2023;41: 1424–1433.
978 doi:10.1038/s41587-023-01674-2

979 132. Weiss AS, Burrichter AG, Durai Raj AC, von Strempel A, Meng C, Kleigrewe K, et al. Exploring
980 the interaction network of a synthetic gut bacterial community. Cold Spring Harbor Laboratory;
981 2021 Feb. doi:10.1101/2021.02.25.432904

982 133. Fernandez-Julia P, Commane DM, van Sinderen D, Munoz-Munoz J. Cross-feeding interactions
983 between human gut commensals belonging to the Bacteroides and Bifidobacterium genera when
984 grown on dietary glycans. Microbiome Res Rep. 2022 [cited 15 Apr 2024].
985 doi:10.20517/mrr.2021.05

986 134. Silverstein RB, Mysorekar IU. Group therapy on in utero colonization: seeking common truths and
987 a way forward. Microbiome. 2021;9. doi:10.1186/s40168-020-00968-w

988 135. Xiao L, Zhao F. Microbial transmission, colonisation and succession: from pregnancy to infancy.
989 Gut. 2023;72: 772–786. doi:10.1136/gutjnl-2022-328970

990 136. Owen RL. Uptake and transport of intestinal macromolecules and microorganisms by M cells in
991 Peyer's patches—a personal and historical perspective. Elsevier; 1999. pp. 157–163.

992 137. Agace WW, McCoy KD. Regionalized Development and Maintenance of the Intestinal Adaptive
993 Immune Landscape. Immunity. 2017;46: 532–548. doi:10.1016/j.immuni.2017.04.004

994 138. Smith P, MacDonald T, Blumberg R. Society for Mucosal Immunology. Principles of mucosal
995 immunology. London: Garland Science. 2013.

996 139. Baptista A, Olivier B, Goverse G, Greuter M, Knippenberg M, Kusser K, et al. Colonic patch and
997 colonic SILT development are independent and differentially regulated events. Mucosal Immunol.
998 2013;6: 511–521.

999 140. Buettner M, Lochner M. Development and function of secondary and tertiary lymphoid organs in
1000 the small intestine and the colon. Front Immunol. 2016;7: 342.

1001 141. Chang S-Y, Cha H-R, Uematsu S, Akira S, Igarashi O, Kiyono H, et al. Colonic patches direct the
1002 cross-talk between systemic compartments and large intestine independently of innate immunity. J
1003 Immunol. 2008;180: 1609–1618.

1004 142. Owen RL, Piazza AJ, Ermak TH. Ultrastructural and cytoarchitectural features of lymphoreticular
1005 organs in the colon and rectum of adult BALB/c mice. Am J Anat. 1991;190: 10–18.

1006 143. Miller H, Zhang J, KuoLee R, Patel GB, Chen W. Intestinal M cells: the fallible sentinels? World J
1007 Gastroenterol WJG. 2007;13: 1477.

1008 144. Shu J-X, Zhong C-S, Shi Z-J, Zeng B, Xu L-H, Ye J-Z, et al. Berberine augments hypertrophy of
1009 colonic patches in mice with intraperitoneal bacterial infection. Int Immunopharmacol. 2021;90:
1010 107242.

1011 145. Dohi T, Rennert PD, Fujihashi K, Kiyono H, Shirai Y, Kawamura YI, et al. Elimination of colonic
1012 patches with lymphotoxin β receptor-Ig prevents Th2 cell-type colitis. J Immunol. 2001;167:
1013 2781–2790.

1014 146. Gibbons D, Spencer J. Mouse and human intestinal immunity: same ballpark, different players;
1015 different rules, same score. Mucosal Immunol. 2011;4: 148–157.

1016 147. Barone F, Patel P, Sanderson J, Spencer J. Gut-associated lymphoid tissue contains the molecular
1017 machinery to support T-cell-dependent and T-cell-independent class switch recombination.
1018 Mucosal Immunol. 2009;2: 495–503. doi:10.1038/mi.2009.106

1019 148. Knoop KA, Newberry RD. Isolated Lymphoid Follicles are Dynamic Reservoirs for the Induction
1020 of Intestinal IgA. Front Immunol. 2012;3. doi:10.3389/fimmu.2012.00084

1021 149. Sollid LM, Iversen R. Tango of B cells with T cells in the making of secretory antibodies to gut
1022 bacteria. Nat Rev Gastroenterol Hepatol. 2022;20: 120–128. doi:10.1038/s41575-022-00674-y

1023 150. Nowosad CR, Mesin L, Castro TBR, Wichmann C, Donaldson GP, Araki T, et al. Tunable
1024 dynamics of B cell selection in gut germinal centres. Nature. 2020;588: 321–326.
1025 doi:10.1038/s41586-020-2865-9

1026 151. Vergani S, Muleta KG, Da Silva C, Doyle A, Kristiansen TA, Sodini S, et al. A self-sustaining
1027 layer of early-life-origin B cells drives steady-state IgA responses in the adult gut. Immunity.
1028 2022;55: 1829-1842.e6. doi:10.1016/j.immuni.2022.08.018

1029 152. Zhao Q, Elson CO. Adaptive immune education by gut microbiota antigens. Immunology.
1030 2018;154: 28–37. doi:10.1111/imm.12896

1031 153. Jackson MA, Pearson C, Ilott NE, Huus KE, Hegazy AN, Webber J, et al. Accurate identification
1032 and quantification of commensal microbiota bound by host immunoglobulins. Microbiome.
1033 2021;9: 1–22.

1034 154. Qian G, Mahdi A. Sensitivity analysis methods in the biomedical sciences. Math Biosci. 2020;323:
1035 108306.

1036 155. Spencer J, Sollid LM. The human intestinal B-cell response. Mucosal Immunol. 2016;9: 1113–
1037 1124.

1038 156. Gullberg E, Keita ÅV, Sa'ad YS, Andersson M, Caldwell KD, Söderholm JD, et al. Identification
1039 of cell adhesion molecules in the human follicle-associated epithelium that improve nanoparticle
1040 uptake into the Peyer's patches. J Pharmacol Exp Ther. 2006;319: 632–639.

1041 157. Hase K, Kawano K, Nochi T, Pontes GS, Fukuda S, Ebisawa M, et al. Uptake through
1042 glycoprotein 2 of FimH+ bacteria by M cells initiates mucosal immune response. Nature.
1043 2009;462: 226–230.

1044 158. Rollenske T, Burkhalter S, Muerner L, von Gunten S, Lukasiewicz J, Wardemann H, et al.
1045 Parallelism of intestinal secretory IgA shapes functional microbial fitness. Nature. 2021;598: 657–
1046 661.

1047 159. Goenka A, Kollmann TR. Development of immunity in early life. J Infect. 2015;71: S112–S120.

1048 160. Hahn A, Thiessen N, Pabst R, Buettner M, Bode U. Mesenteric lymph nodes are not required for
1049 an intestinal immunoglobulin A response to oral cholera toxin. Immunology. 2010;129: 427–436.

1050 161. Rios D, Wood M, Li J, Chassaing B, Gewirtz A and, Williams I. Antigen sampling by intestinal M
1051 cells is the principal pathway initiating mucosal IgA production to commensal enteric bacteria.
1052 Mucosal Immunol. 2016;9: 907–916.

1053 162. Li C, Lam E, Perez-Shibayama C, Ward LA, Zhang J, Lee D, et al. Early-life programming of
1054 mesenteric lymph node stromal cell identity by the lymphotoxin pathway regulates adult mucosal
1055 immunity. Sci Immunol. 2019;4: eaax1027.

1056 163. Hashizume-Takizawa T, Shibata N, Kurashima Y, Kiyono H, Kurita-Ochiai T, Fujihashi K.
1057 Distinct roles for Peyer's patch B cells for induction of antigen-specific IgA antibody responses in
1058 mice administered oral recombinant Salmonella. Int Immunol. 2019;31: 531–541.

1059 164. Hashizume-Takizawa T, Kobayashi R, Tsuzukibashi O, Saito M, Kurita-Ochiai T. CCR7-deficient
1060 mice exhibit a delayed antigen-specific mucosal IgA antibody response to an oral recombinant
1061 Salmonella strain. Pathog Dis. 2019;77: ftz024.

1062 165. Wieland CW, Koppel EA, den Dunnen J, Florquin S, McKenzie AN, van Kooyk Y, et al. Mice
1063 lacking SIGNR1 have stronger T helper 1 responses to Mycobacterium tuberculosis. Microbes
1064 Infect. 2007;9: 134–141.

1065 166. Chardin H, Mercier K, Frydman C, Vollmer N. Surface plasmon resonance imaging: a method to
1066 measure the affinity of the antibodies in allergy diagnosis. J Immunol Methods. 2014;405: 23–28.

1067 167. Schasfoort RB, van Weperen J, van Amsterdam M, Parisot J, Hendriks J, Koerselman M, et al.
1068 Presence and strength of binding of IgM, IgG and IgA antibodies against SARS-CoV-2 during
1069 CoViD-19 infection. Biosens Bioelectron. 2021;183: 113165.

1070 168. Noy-Porat T, Alcalay R, Mechaly A, Peretz E, Makdasi E, Rosenfeld R, et al. Characterization of
1071 antibody-antigen interactions using biolayer interferometry. STAR Protoc. 2021;2: 100836.

1072 169. Huang Y, Chen Z, Wang H, Ba X, Shen P, Lin W, et al. Follicular regulatory T cells: a novel
1073 target for immunotherapy? Clin Transl Immunol. 2020;9: e1106.

1074 170. Wing JB, Ise W, Kurosaki T, Sakaguchi S. Regulatory T cells control antigen-specific expansion
1075 of Tfh cell number and humoral immune responses via the coreceptor CTLA-4. Immunity.
1076 2014;41: 1013–1025.

1077 171. Zotos D, Coquet JM, Zhang Y, Light A, D'Costa K, Kallies A, et al. IL-21 regulates germinal
1078 center B cell differentiation and proliferation through a B cell–intrinsic mechanism. J Exp Med.
1079 2010;207: 365–378.

1080 172. El Shikh MEM, El Sayed R, Aly NAR, Prediletto E, Hands R, Fossati-Jimack L, et al. Follicular
1081 dendritic cell differentiation is associated with distinct synovial pathotype signatures in rheumatoid
1082 arthritis. Front Med. 2022;9: 1013660.

1083 173. Haniuda K, Nojima T, Kitamura D. In vitro-induced germinal center b cell culture system.
1084 Germinal Cent Methods Protoc. 2017; 125–133.

1085 174. Huang X, Yang W, Yao S, Bilotta AJ, Lu Y, Zhou Z, et al. IL-21 promotes intestinal memory IgA
1086 responses. J Immunol. 2020;205: 1944–1952.

1087 175. Lei X-F, Ohkawara Y, Stämpfli MR, Mastruzzo C, Marr RA, Snider D, et al. Disruption of
1088 antigen-induced inflammatory responses in CD40 ligand knockout mice. J Clin Invest. 1998;101:
1089 1342–1353.

176. Xu J, Foy TM, Laman JD, Elliott EA, Dunn JJ, Waldschmidt TJ, et al. Mice deficient for the CD40 ligand. Immunity. 1994;1: 423–431.

177. Purwada A, Shah SB, Béguelin W, August A, Melnick AM, Singh A. Ex vivo synthetic immune tissues with T cell signals for differentiating antigen-specific, high affinity germinal center B cells. Biomaterials. 2019;198: 27–36.

178. Purwada A, Jaiswal MK, Ahn H, Nojima T, Kitamura D, Gaharwar AK, et al. Ex vivo engineered immune organoids for controlled germinal center reactions. Biomaterials. 2015;63: 24–34.

179. Corinaldesi C, Holmes AB, Shen Q, Grunstein E, Pasqualucci L, Dalla-Favera R, et al. Tracking immunoglobulin repertoire and transcriptomic changes in germinal center B cells by single-cell analysis. Front Immunol. 2022;12: 818758.

180. Biram A, Shulman Z. Evaluation of B cell proliferation in vivo by EdU incorporation assay. Bio-Protoc. 2020;10: e3602–e3602.

Acknowledgments:
We are grateful to Prof. Dr. Emma Slack and Prof. Dr. M.D. Mathias Hornef for their valuable time and insightful discussions, which significantly improved our work.

Funding:
SNSF postdoc.mobility grant P500PB_206889 (BT)
Branco Weiss Fellowship—Society in Science administered by the ETH Zurich and Rutgers Cancer Institute of New Jersey New Investigator Award (AIL)
N/A (CJEM)

Authors contributions:
Conceptualization: BT, AIL, CJEM
Data curation: BT
Methodology: BT, CJEM
Formal Analysis: BT, CJEM
Visualization: BT
Software: BT
Supervision: AIL, CJEM
Writing – original draft: BT, CJEM
Writing – review & editing: BT, AIL, CJEM

Competing interests: The authors declare that they have no competing interests.
Materials & Correspondence: Correspondence and material requests should be addressed to Burcu Tepekule.

Data and materials availability: All data and code used in this work is available at https://github.com/burcutepekule/ONIMTOL under the GNU General Public License v3.0.

Supplementary Materials
Materials and Methods

Supplementary Text
Figs. S1 to S11
Tables S1 to S6
References (80–180)

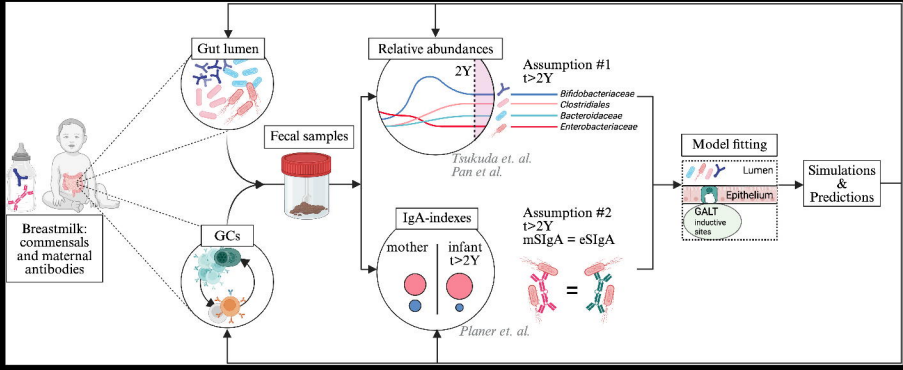
Breastmilk: commensals and maternal antibodies
Gut lumen
GCs
Fecal samples
Relative abundances
2Y
Assumption #1
t>2Y
Bifidobacteriaceae
Clostridiales
Bacteroidaceae
Enterobacteriaceae
Tsukuda et. al.
Pan et al.
IgA-indexes
mother
infant
t>2Y
Planer et. al.
Assumption #2
t>2Y
mSIgA = eSIgA
=
Model fitting
Lumen
Epithelium
GALT inductive sites
Simulations & Predictions

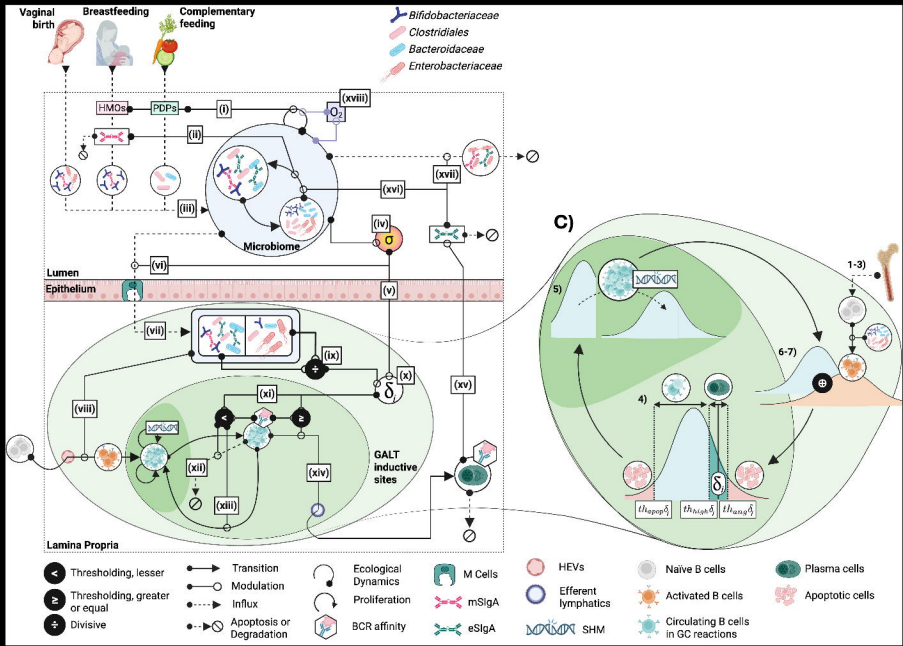
Vaginal birth
Breastfeeding
Complementary feeding
Bifidobacteriaceae
Clostridiales
Bacteroidaceae
Enterobacteriaceae
HMOs
PDPs
(i)
(ii)
(iii)
(iv)
(v)
(vi)
(vii)
(viii)
(ix)
(x)
(xi)
(xii)
(xiii)
(xiv)
(xv)
(xvi)
(xvii)
(xviii)
Microbiome
Lumen
Epithelium
GALT inductive sites
Lamina Propria
C)
1-3)
4)
5)
6-7)
Thresholding, lesser
Thresholding, greater or equal
Divisive
Transition
Modulation
Influx
Apoptosis or Degradation
Ecological Dynamics
Proliferation
BCR affinity
M Cells
mSIgA
eSIgA
HEVs
Efferent lymphatics
SHM
Naive B cells
Activated B cells
Circulating B cells in GC reactions
Plasma cells
Apoptotic cells

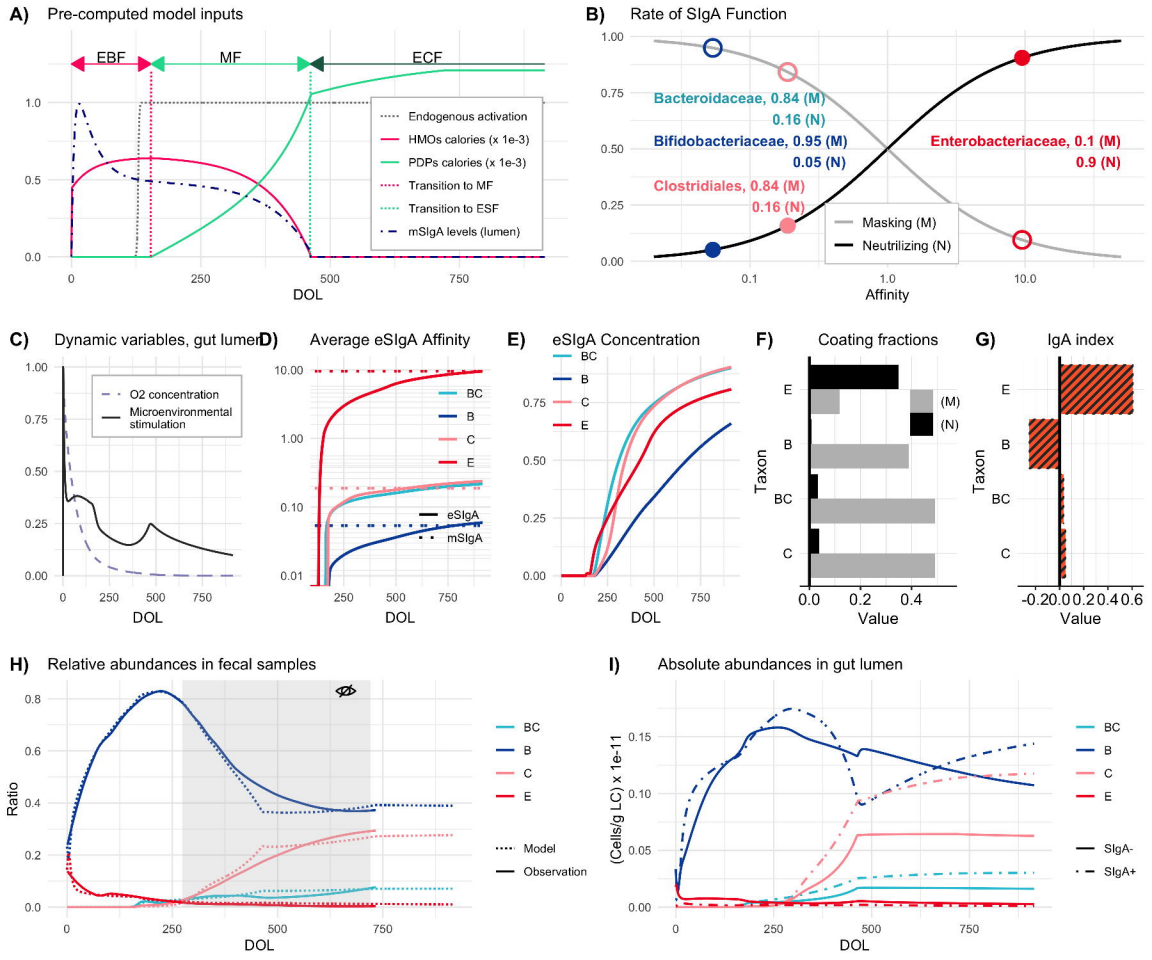
A)
Pre-computed model inputs
EBF
MF
ECF
Endogenous activation
HMOs calories (x 1e-3)
PDPs calories (x 1e-3)
Transition to MF
Transition to ESF
mSIgA levels (lumen)
DOL
B)
Rate of SIgA Function
Bacteroidaceae, 0.84 (M)
0.16 (N)
Bifidobacteriaceae, 0.95 (M)
0.05 (N)
Clostridiales, 0.84 (M)
0.16 (N)
Enterobacteriaceae, 0.1 (M)
0.9 (N)
Masking (M)
Neutrilizing (N)
Affinity
C)
Dynamic variables, gut lumen
O2 concentration
Microenvironmental stimulation
DOL
D)
Average eSIgA Affinity
BC
B
C
E
eSIgA
mSIgA
DOL
E)
eSIgA Concentration
BC
B
C
E
DOL
F)
Coating fractions
Taxon
(M)
(N)
Value
G)
IgA index
Taxon
Value
H)
Relative abundances in fecal samples
Ratio
BC
B
C
E
Model
Observation
DOL
I)
Absolute abundances in gut lumen
(Cells/g LC) x 1e-11
BC
B
C
E
SIgA-
SIgA+
DOL

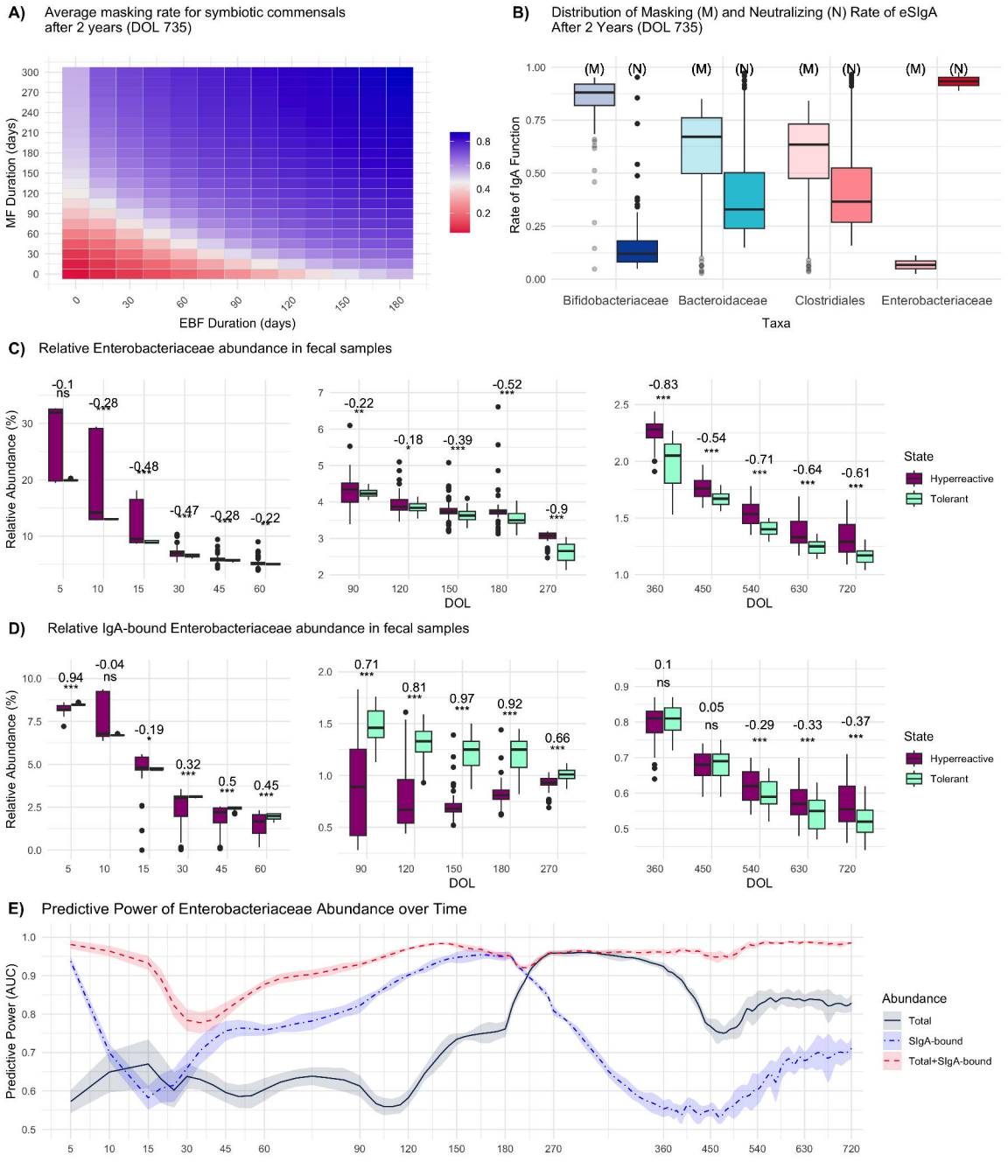
A)
Average masking rate for symbiotic commensals after 2 years (DOL 735)
MF Duration (days)
EBF Duration (days)
B)
Distribution of Masking (M) and Neutralizing (N) Rate of eSIgA After 2 Years (DOL 735)
Rate of IgA Function
Bifidobacteriaceae
Bacteroidaceae
Clostridiales
Enterobacteriaceae
Taxa
C)
Relative Enterobacteriaceae abundance in fecal samples
Relative Abundance (%)
DOL
State
Hyperreactive
Tolerant
D)
Relative IgA-bound Enterobacteriaceae abundance in fecal samples
Relative Abundance (%)
DOL
State
Hyperreactive
Tolerant
E)
Predictive Power of Enterobacteriaceae Abundance over Time
Predictive Power (AUC)
Abundance
Total
SIgA-bound
Total+SIgA-bound

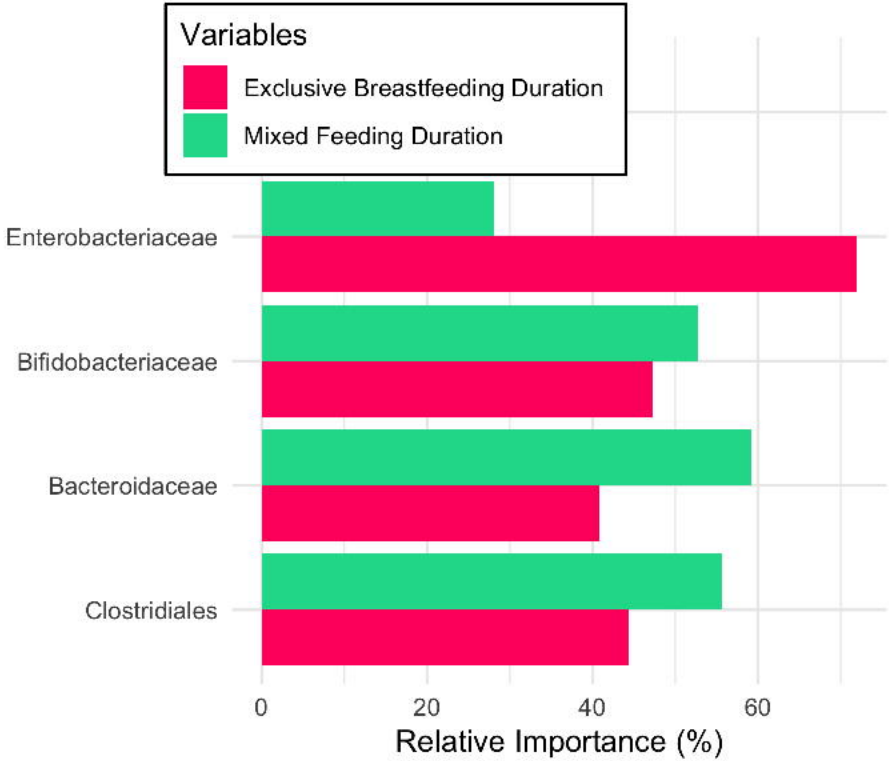
Variables
Exclusive Breastfeeding Duration
Mixed Feeding Duration
Enterobacteriaceae
Bifidobacteriaceae
Bacteroidaceae
Clostridiales
0
20
40
60
Relative Importance (%)

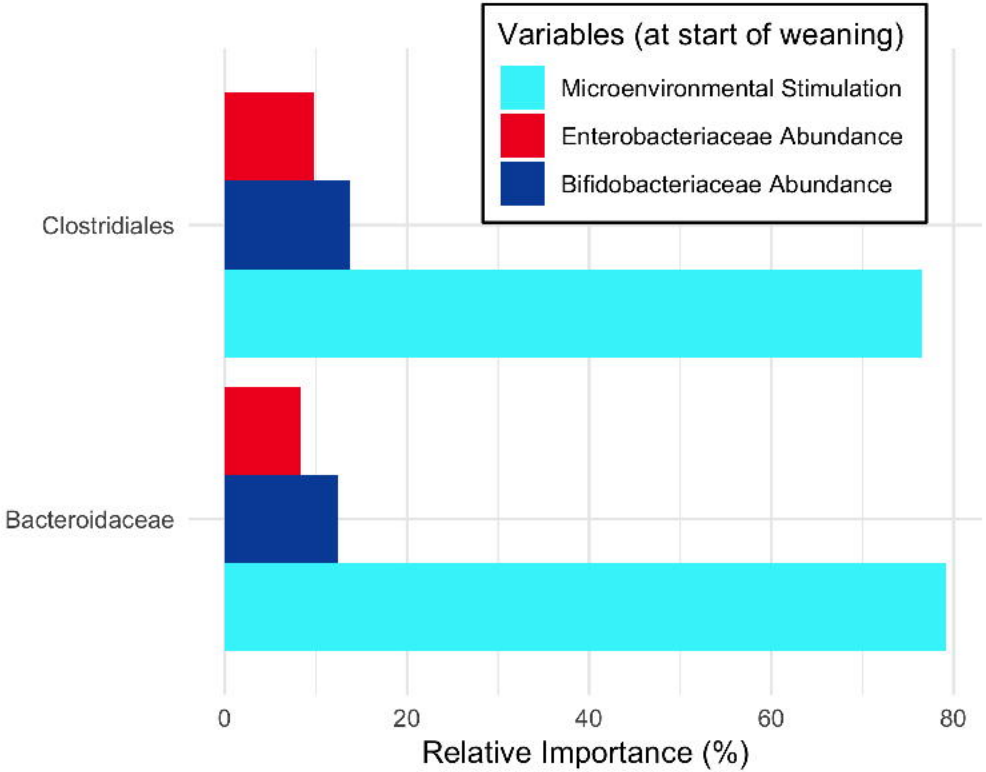
Variables (at start of weaning)
Microenvironmental Stimulation
Enterobacteriaceae Abundance
Bifidobacteriaceae Abundance
Clostridiales
Bacteroidaceae
0
20
40
60
80
Relative Importance (%)

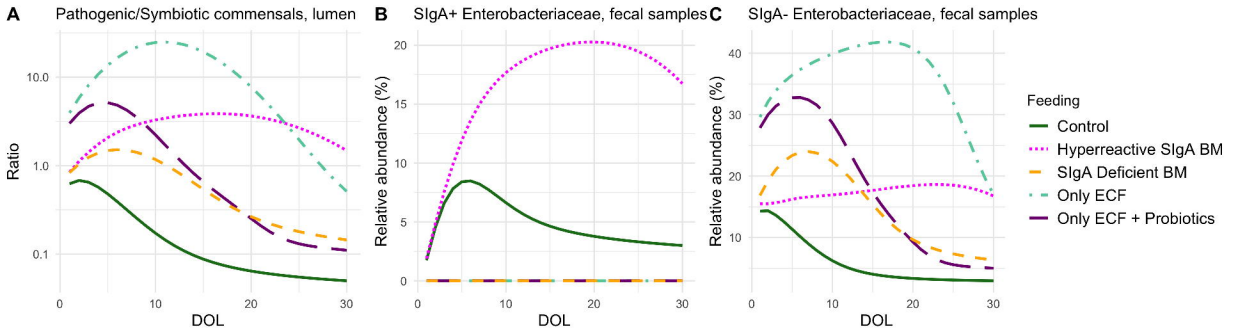
A
Pathogenic/Symbiotic commensals, lumen
Ratio
10.0
1.0
0.1
0
10
20
30
DOL
B
SIgA+ Enterobacteriaceae, fecal samples
Relative abundance (%)
20
15
10
5
0
0
10
20
30
DOL
C
SIgA- Enterobacteriaceae, fecal samples
Relative abundance (%)
40
30
20
10
0
10
20
30
DOL
Feeding
Control
Hyperreactive SIgA BM
SIgA Deficient BM
Only ECF
Only ECF + Probiotics